Ref. Ares(2013)3544342 - 22/11/2013

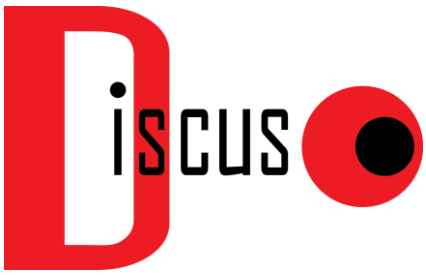

D4.1

Assessment of advanced LR-PON transmission technologies

Dissemination Level: PU

- **Dissemination level:**

  PU = Public,
  RE = Restricted to a group specified by the consortium (including the Commission Services),
  PP = Restricted to other programme participants (including the Commission Services),
  CO = Confidential, only for members of the consortium (including the Commission Services)

Abstract:

This deliverable assesses various advanced LR-PON transmission schemes from a top-level system point-of-view. It focuses on multi-wavelength hybrid TDM/WDM LR-PONs and system requirements for the key components to be developed within DISCUS (e.g. tuneable components, burst-mode EDC, 40G single-carrier downstream upgrade scheme). In addition, a coherent optical access system (WDM LR-PON) and alternative modulation and multiplexing schemes (OOFDM and subcarrier multiplexing) are investigated.

(M11, ALUD, Tyndall, III-V, COR, ASTON, editor IMEC, dissemination level: Public).

Authors:

Name	Affiliation
Xin (Scott) Yin	IMEC
Xing-Zhi Qiu	IMEC
Wolfgang Poehlmann	ALUD
Thomas Pfeiffer	ALUD
Harald Rohde	COR
Romain Brenot	III-V
Mohand Achouche	III-V
Peter Ossieur	Tyndall
Brendan Roycroft	Tyndall
Giuseppe Talli	Tyndall
Elias Gaikoumidis	ASTON
Farsheed Farjady	ASTON

Due Date: 30.9.2013

COPYRIGHT

© Copyright by the DISCUS Consortium.

The DISCUS Consortium consists of:

Participant Number	Participant organization name	Participant org. short name	Country
Coordinator			
1	Trinity College Dublin	TCD	Ireland
Other Beneficiaries			
2	Alcatel-Lucent Deutschland AG	ALUD	Germany
3	Coriant GmbH	COR	Germany
4	Telefonica Investigacion Y Desarrollo SA	TID	Spain
5	Telecom Italia S.p.A	TI	Italy
6	Aston University	ASTON	United Kingdom
7	Interuniversitair Micro-Electronica Centrum VZW	IMEC	Belgium
8	III V Lab GIE	III-V	France
9	University College Cork, National University of Ireland, Cork	Tyndall & UCC	Ireland
10	Polatis Ltd	POLATIS	United Kingdom
11	atesio GMBH	ATESIO	Germany
12	Kungliga Tekniska Hoegskolan	KTH	Sweden

This document may not be copied, reproduced, or modified in whole or in part for any purpose without written permission from the DISCUS Consortium. In addition to such written permission to copy, reproduce, or modify this document in whole or part, an acknowledgement of the authors of the document and all applicable portions of the copyright notice must be clearly referenced.

All rights reserved.

TABLE OF CONTENTS

1 INTRODUCTION 7

2 MULTI-WAVELENGTH HYBRID TDM/WDM LR-PONS 7

2.1 SYSTEM REQUIREMENTS FOR THE MULTI-WAVELENGTH HYBRID TDM/WDM LR-PONS 7

2.1.1 NG-PON2 Technology Evaluation 7

2.1.2 NG-PON2 Wavelength Plan 8

2.1.3 NG-PON2 TWDM Optical Budget Classes 10

2.1.4 Relevance of NG-PON2 for DISCUS 13

2.1.5 Special aspects of wavelength control in TWDM PON and mitigation of rogue behavior 13

2.2 TUNABLE LASERS 14

2.3 TUNABLE FILTER 16

2.4 BURST-MODE ELECTRONIC DISPERSION COMPENSATION 20

2.4.1 Need for burst-mode electronic dispersion compensation 20

2.4.2 The linear burst-mode receiver 21

2.4.3 High-level architectural considerations on the BM-EDC 22

2.4.4 Transmission performance of the mixed-signal approach 22

2.4.5 Convergence of the tap adaptation algorithm 24

2.4.6 Conclusion 25

2.5 SINGLE CARRIER 40GBIT/S DOWNSTREAM UPGRADE SCHEME 25

2.5.1 OSNR requirements for 3-level duobinary modulation 26

2.5.2 Power budget and OSNR modelling of 40Gbit/s downstream 29

2.5.3 Dispersion penalty 33

2.5.4 Conclusion 35

3 COHERENT DETECTION SCHEME (WDM LR-PON) 36

3.1 SYSTEM DESIGN AND CAPABILITIES 36

3.2 BASIC WORKING PRINCIPLE: PAIRED CHANNEL TECHNOLOGY 37

3.3 CLOCKS, FREQUENCIES AND FREQUENCY RELATIONS 39

3.4 BIT RATE FLEXIBILITY 39

3.5 REAL TIME OLT 40

3.6 REAL TIME ONU 42

3.7 WAVELENGTH ASSIGNMENT 43

3.8 SYSTEM CAPABILITIES ENABLED BY WAVELENGTH FLEXIBILITY 44

4 DIRECT DETECTION AND COHERENT OPTICAL OFDM 45

4.1 OPTICAL OFDM 45

4.1.1 Intensity-Modulation 46

4.1.2 Field-Modulation 47

4.1.3 Direct-Detection Optical OFDM (DD-OOFDM) 48

4.1.4 Coherent Optical OFDM (CO-OFDM) 48

4.1.5 Comparison between CO-OFDM and DD-OOFDM 50

4.2 OPTICAL OFDM FOR LONG-REACH PON 51

4.2.1 100 Gbit/s downstream CO-OFDM 52

4.2.2 Direct-Detected LR-OFDM PON using Cost-Effective High-speed GaAs IQ Electro-Optic Modulators 53

4.3 TECHNO-ECONOMIC OFDM MODEL AND COMPARISONS WITH LEGACY PONS 57

5 REFERENCES 61

6 ABBREVIATIONS 66

1 Introduction

One of the main objectives of WP4 is to identify an efficient integrated optical access network architecture supporting the end-to-end approach of DISCUS. The metro/access section of the DISCUS network is built on long reach PON (LR-PON) solutions. This deliverable assesses various advanced LR-PON transmission schemes from a top-level system point-of-view. Therefore this deliverable includes:

Section 2 describes the design guidelines and system requirements for a multi-wavelength TDM/WDM LR-PON network. The hybrid TDM/WDM LR-PON in DISCUS is a network with 10Gbit/s or high rate (up to 40Gbit/s) per wavelength in the C-band and reaching out to typically 256 users at up to 100 km distance. Various system requirements for the key components, such as tuneable lasers, tuneable filters, burst-mode receiver and electronic dispersion compensation, are identified. Moreover, an upgrade path to higher rate per wavelength is being investigated and will be evaluated for the data rate up to 40Gbit/s.

A coherent optical access system which is able to deliver an individual wavelength to a high number (up to 1000) users is described in Section 3. This section gives an overview of the capabilities, design and implementation of a coherent ultra dense WDM technology for LR-PON networks. A number of attractive options, such as a wide range of downstream bit rates, and the coexistence with existing systems are discussed in details.

In Section 4 optical orthogonal frequency division multiple (OFDM) is be investigated for bit-rates up to 100 Gbit/s in the LR-PON configurations of D2.1, namely, the basic LR-PON design with single fibre working in ODN and two fibre working in the backhaul, and the LR-PON architecture with two fibre working in both the ODN and backhaul for different type of amplifiers. Finally, the techno-economic aspect of direct detection and coherent detection optical OFDM is briefly discussed with the LR-PON architecture.

In WP4, the detailed specifications of DISCUS LR-PON implementation will be investigated further and presented in a second deliverable D4.2 “System specifications for LR-PON implementation” (M13).

2 Multi-wavelength Hybrid TDM/WDM LR-PONs

2.1 System requirements for the multi-wavelength hybrid TDM/WDM LR-PONs

2.1.1 NG-PON2 Technology Evaluation

FSAN, the Full Service Access Networks group investigated different technological options for the next generation of PONs (NG-PON2). The basic requirements were to supply a minimum of 40 Gbit/s for downstream and 10 Gbit/s for upstream at a reach of up to 40km and a minimum optical path loss of 29dB. Co-existence with already deployed technologies is required.

For a detailed study four candidate technologies were techno-economically evaluated. The first technology under consideration was a TDM-PON with increased up and downstream bit rate (XLG-PON). This is basically an extension of the technology of already deployed PON systems (e. g. G-PON, EPON, XG-PON1, 10G-EPON). To overcome issues of the high downstream bit rate, duo binary transmission is proposed for the 40 Gbit/s downstream in the O-band.

The second proposal was TWDM-PON, reusing most of the electronics of XG-PON1 for 10Gbit/s downstream and 2.5Gbit/s upstream. The required bitrates for NG-PON2 were achieved by operating 4 channels in a low cost WDM scheme. The binary signal is a scrambled NRZ.

The third proposal covered several flavours of WDM technologies. Specifically external seeded, wavelength reuse and tuneable WDM PON were the more traditional in scope solutions. Ultra-dense (coherent) and self-seeded WDM were evaluated as solutions with new aspects. In contrast to the TWDM approach, a higher number of WDM channels were considered with lower bitrates on each channel.

In the forth proposal, OFDM technologies were studied in coherent and direct detection schemes.

The decision on the technologies for NG-PON2 was taken on the Bath meeting in April 2012. TWDM-PON was selected as primary solution and an optional WDM overlay was included. The TDM part of TWDM PON is kept similar as in XG-PON1, the preceding technology. The downstream is a continuous TDM signal and the upstream is a burst mode time division multiple access (TDMA) signal.

All results and parameters given in this section reflect the current status of discussion in FSAN. This can be taken as a basis for the work in DISCUS, but should not be understood as a limitation.

2.1.2 NG-PON2 Wavelength Plan

One requirement for NG-PON2 was the coexistence with legacy PON systems as G-PON and XG-PON1 on the same optical distribution network (ODN). This was ensured by a co-existence element (see Figure 1) and a proper definition of the wavelength plan (see Figure 2). The co-existence element is an optical filter.

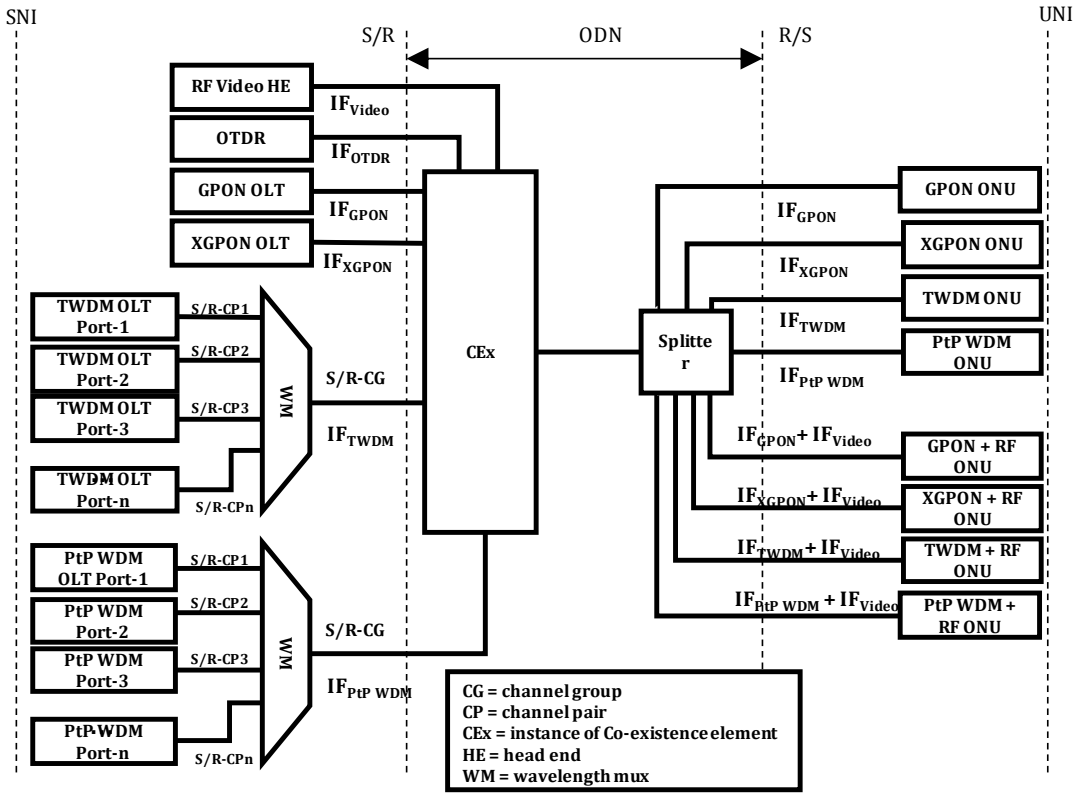

Figure 1 Concept of co-existence for NG-PON2 [1]

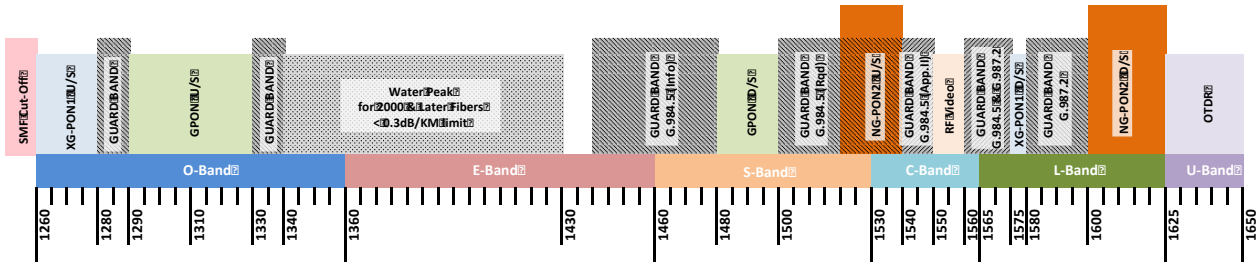

Figure 2 Wavelength plan for NG-PON2 [1]

For the downstream (D/S) a 100GHz based DWDM grid is defined starting from 1596.34nm. The baseline is four channel pairs, but it could be extended up to eight channel pairs. A typical implementation might be externally modulated transmitters in the optical line terminal (OLT) and a low cost tuneable optical filter in the optical network unit (ONU).

For the upstream (U/S) 1524 – 1544nm is used as wide range and 1524-1540nm as narrow range band. For this band the grid can be anything between 50 and 100 GHz. The assignment of channels can be either by wavelength bands or wavelength-sets [2].

For the point to point WDM overlay, the wavelength plan is defined as in Table 1. Two options are given: in the shared spectrum case, TWDM and p2p WDM overlay share one fiber (and therefore the available spectrum). In the full

spectrum case, the fiber is only used by the p2p WDM system and therefore the full spectrum from 1524 to 1625 nm can be used. The channel spacing can be based on 50GHz or 100GHz DWDM.

Table 1 wavelength plan for TWDM and the p2p WDM overlay.

Wavelength / **Compatible Systems**	**TWDM**		**PtP WDM**
	DS	**US**	US/DS
GPON, RF Video, XG-PON1	1596-1603 nm	Wide Range 1524-1544 nm Narrow Range 1524-1540 nm	Shared Spectrum 1603-1625 nm Full Spectrum 1524-1625 nm

The following text describes the coexistence choices and is copied from the current draft of G.989.2:

> *This recommendation recognizes PtP WDM spectrum anywhere in the spectrum identified subject to spectrum otherwise assigned or in use for transmission or guard-bands. Whenever a particular subset of the spectrum in either band is unused by TWDM and/or legacy system according to the NG-PON2 wavelength plan, PtP WDM shall be permitted to make use of that particular sub-band in upstream and/or downstream direction, subject to the isolation requirements of the legacy systems. When TWDM and PtP WDM are both present, wavelength channels of both technologies can occupy adjacent frequency grids, note that TWDM and PtP WDM channels are not allowed to be interleaved. The required guard band between TWDM and PtP WDM is a minimum of 3 nm when using a separate WM, and is included in the band definitions. When using a shared WM between PtP WDM and TWDM, the required guard band is a minimum of 100 GHz.*

2.1.3 NG-PON2 TWDM Optical Budget Classes

The optical budget is given by the difference of transmitter power (PTX) and receiver sensitivity (P_{RX}) reduced by the optical path penalty (OPP). A forward error correction (FEC) code is used with an input bit error rate (BER) of 1e-4 for 2.5Gbit/s and 1e-3 for 10Gbit/s. For the 10 Gbit/s downstream an OPP of up to 2dB is assumed. For the 2.5Gbit/s upstream, the OPP ranges from 1dB (N1 and N2, 20km) up to 2dB (E1 and E2, 40km). The main cause of this range is Raman interaction.

Table 2 Budget classes as defined in G.989.2

	N1	N2	E1	E2
Minimum loss	14dB	16dB	18dB	20dB
Maximum loss	29dB	31dB	33dB	35dB

The budget classes are defined as shown in Table 2. The minimum loss is always 15dB less than the maximum loss, what should reflect different link length and splitter levels. The budget is used for the compensation of the loss of the coexistence filter, the fiber, splitter, connectors and splices.

The general strategy for cost effective PONs is to make the ONU as cheap as possible. Therefore the P_{RX} for the 10Gbit/s downstream is -28dBm for all budget classes (see Table 3), what can be achieved by an APD with a tunable optical filter. The minimum P_{TX} for the 2.5Gbit/s upstream is 0dBm for the case of preamplified receivers in the OLT and +4dBm for unamplified receivers in the OLT (see Table 4). This is also true for all budget classes. There is as well a 10Gbit/s upstream option. For unamplified receivers only N1 and N2 will be supported with a P_{TX} of +4dBm. The maximum P_{TX} is always 5 dB higher than the minimum, to keep the optical power control circuit simple. A thermal tuned DFB laser is the most likely solution for the ONU transmitter at 2.5Gbit/s.

This way of definition has on one side the advantage that there will be a high volume of just one type of ONU. Furthermore an upgrade from one budget class to another will be possible by just changing the OLT equipment and leaving all the ONUs unchanged.

Table 3 Downstream TWDM transmitter and receiver parameters

10Gbit/s downstream					
OLT transmitter					
		N1	**N2**	**E1**	**E2**
Mean launch power Min. (at SR/CG)	dBm	+3	+5	+7	+9
Mean launch power Max. (at SR/CG)	dBm	+7	+9	+11	+11
ONU receiver					
Max optical path penalty	dB	2			
BER reference level		1e-3			
Minimum sensitivity at BER ref.	dBm	-28	-28	-28	-28
Minimum overload at BER ref.	dBm	-7	-7	-7	-9

Table 4 Upstream TWDM transmitter and receiver parameters

2.5 Gbit/s upstream					
ONU transmitter					
		N1	**N2**	**E1**	**E2**
Mean launch power Min.					
-amplified OLT RX	dBm	0	0	0	0
-unamplified OLT RX	dBm	+4	+4	+4	+4
Mean launch power Max.					
-amplified OLT RX	dBm	+5	+5	+5	+5
-unamplified OLT RX	dBm	+9	+9	+9	+9
OLT receiver					
Max optical path penalty	dB	???			
BER reference level		1e-4			
Min. sensitivity at BER reference (at SR/CG)					
-unamplified OLT RX	dBm	-26	-28	-30.5	-32.5
-amplified OLT RX	dBm	-30	-32	-34.5	-36.5
Max overload at BER reference (at SR/CG)					
-unamplified OLT RX	dBm	-5	-5	-5	-5
-amplified OLT RX	dBm	-9	-9	-9	-9

For the TWDM OLT the minimum downstream P_{TX} is defined as +3dBm (N1), up to +9dBm (E2). The maximum P_{TX} is always 4dB higher, because for the OLT side a more complex power level control can be afforded. For the OLT transmitters an externally modulated laser is a likely solution, possibly with a booster amplifier. The OLT receiver consists of a preamplifier (in case of amplified receiver) and the wavelength demultiplexer followed by a PIN or APD receiver.

2.1.4 *Relevance of NG-PON2 for DISCUS*

This chapter 2.1 describes the status of I-TUT standardization of a PON system that is optimized for today's network hierarchies with a relative short reaching, moderate split factor optical access networks with OEO conversion to the metro section. For use in a largely optically transparent DISCUS network, a similar system would have different constrains due to e.g. longer reach, inline amplification and better spectral efficiency. Therefore the parameters of a DISCUS compliant NGPON-2 system can be quite different from the actual standards. It should be understood as a starting point, but not as a binding requirement for DISCUS.

2.1.5 *Special aspects of wavelength control in TWDM PON and mitigation of rogue behavior*

Aside from management aspects (wavelength assignment and control), the requirement for a non-wavelength-routing ODN has some ramifications on the operation of the multi wavelength PON, specifically on the ONU transceiver module and on the OLT architecture. It must be ensured that the optical emission on one channel does not interfere with the emission on any other of the WDM channels (linear crosstalk). In downstream direction the WM filter ensures that only the correct wavelength can be injected into the ODN. In upstream direction there is no such filter in the ODN. So special care must be taken that the ONU lasers emit only when

- they are tuned to the correct wavelength or
- the ONU transceiver module includes an optical transmit filter for the correct channel or
- there is no traffic on the network other than control and management signals

Ensuring the correct wavelength setting of a laser before it is turned on requires either a very demanding optical set-up or a precise multi-parameter calibration during production. While this may be tolerable for the high speed channels in the DWDM-PON subsystem, this is generally not compliant with the ultra-low cost targets for the TWDM-PON subsystem. The same is true for the integrated transmit filter in the ONU module.

From a cost perspective the most promising approach is to set the ONU wavelength during a quiet window, e.g. a ranging window in the TWDM-PON, and continuously control the setting end-to-end during operation leveraging the WM-filter in the OLT [3]. For this purpose the ranging windows must be synchronized across all wavelength channels on a given ODN such that the virtual upstream frame is identical for all of them on an absolute time scale. Therefore, the TC/MAC layers of the respective OLT ports must be coordinated in a suitable way.

2.2 Tunable lasers

The laser in the ONU, which acts as the light source for the upstream transmission, needs to tune to the 50 GHz ITU-T grid over at least half the C-band (half of the C-band is assigned to the upstream channels and the other half to the downstream,). While fast (sub-μs scale) tuning speed is not required for the proposed DISCUS network architecture, an important requirement is the need for the laser wavelength to be accurately set within the bandwidth of the assigned channel when the ONU output is active for transmission, in order not to interfere with the traffic of other PON channels (as discussed in section 2.1.5). This means that when an ONU is first connected to the network it has to tune to its assigned upstream wavelength (or within the bandwidth of the assigned channel) without interfering with the traffic of other ONUs and it should remain within the assigned channel bandwidth when the ONU is not transmitting.

It should be also remembered that the transmitter module should be able to blank the output power to very low levels of light in order to avoid interference with the traffic of other users at the same channel or of other channels when tuning. For example in [4] the off-state ONU output power required to achieve a BER better than 10^{-4} for a long-reach PON with a split ratio of 512 is -48.5dBm. This is a very low level of power, which could be challenging to achieve. The use of an SOA as an optical gate at the output of the ONU transmitter has been shown capable to achieve the required levels of off-state suppression within the timescales of the inter-burst guard-band [5]. The use of an SOA as a gating element at the output of the transmitter has also the advantage that the laser section can be maintained with the power on and tuned at the right wavelength even when the ONU is not transmitting.

Additional design parameters are sufficiently narrow linewidth to enable 10 Gbit/s transmission over up to 100 km standard single- mode fibre (less than a few 100MHz), single-mode operation with sufficient side-mode suppression ratio (>25dB), and an overall transmitter output power of +5dBm [6]. These requirements need to be met within the low cost target for the ONT.

When considering different tuneable laser technologies with respect to their cost, one must consider manufacturing costs, test and characterization costs, as well as the production yield. Indeed, compared to traditional applications for tuneable lasers in metro and long-haul networks, volumes for optical access will be several orders of magnitude larger, requiring potentially millions of manufactured devices per annum. Hence, yield, testing and characterization time become important considerations.

Tuneable laser technologies can be broadly classified into three categories: 1) external cavity lasers (ECL), 2) DFB laser arrays and 3) monolithic multi-section designs [7]. Different types of tuneable ECLs have been described [8]. In its most simple form, an ECL consists of a gain element (usually an SOA), a wavelength selective element and mirrors (which may or may not be integrated into either the gain element and the wavelength selective element) [6]. In DFB laser arrays wavelength selection can be achieved using for example a coupler (which results in large coupling losses) [9], or an external micro-mechanical mirror [10]. A drawback of this device is that to ensure coverage of the required wavelength

band, individual DFB lasers may need to be specifically selected, which becomes impractical and costly for high volumes.

Monolithic tuneable lasers have the potential to achieve the lowest manufacturing cost (provided sufficient yield from an individual wafer can be obtained), and also have better prospect in terms of photonic integration with the other ONU components. Commercially available monolithic tuneable lasers are typically variants of the distributed Bragg reflector (DBR) laser, such as for example the sample grating [11], super structure grating [12] and digital supermode DBR lasers [13]. Other types such as the modulated grating Y-branch (MGY) laser are based on interferometric principles using integrated Mach-Zehnder modulators and Y-couplers [14].

Within DISCUS the requirements posed on the tuneable laser are addressed by the study and development of a monolithic tuneable laser based on slotted Fabry-Perot (SFP) designs [15]. Some advantages of SFP lasers over other monolithic tuneable lasers [11][12][13][14] are that they require only a single epitaxial growth, are fully and easily integrated with other photonic components (such as amplifiers or modulators), and require minimal fabrication complexity.

Within Discus, we have recently developed lasers where any remaining facets are defined lithographically, so that there are minimal dimensional variations across similar lasers. These approaches should be compatible with eventual processing of the devices in a foundry. Various device designs are presently being simulated and will be fabricated to support the Discus frequency grid spacing and wavelength coverage. Figure 3 shows an example of the wavelength coverage of an SFP device (fabricated previously to DISCUS), where we can see the coverage of roughly the upper half of the C-band and part of the L-band on a 100GHz grid. Following from this, new designs incorporating an integrated modulator and amplifier will be processed, which will allow data to be transmitted at optimum data rates and power levels for the Discus network. In order to increase energy efficiency and reduce running costs for the consumer, consideration will be given to making the lasers athermal, with the aim of designing lasers that do not require thermo-electric controllers. Successfully fabricated lasers will be packaged into the ONU burst-mode transmitter for system testing.

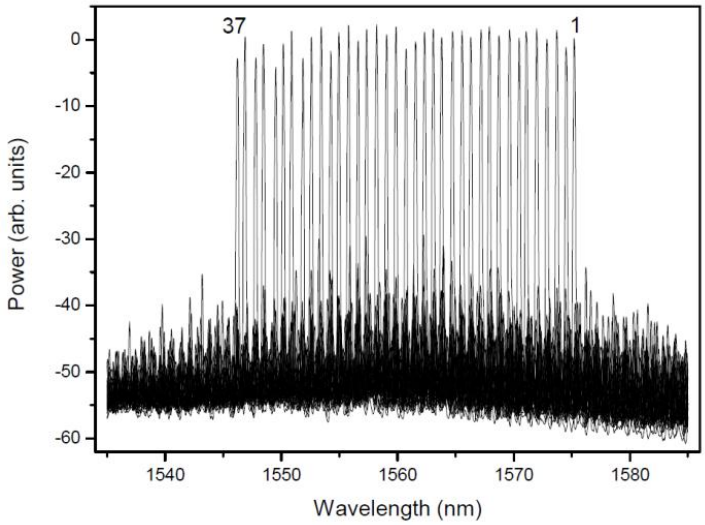

Figure 3 Tunable coverage from a slotted Fabry-Perot laser.

2.3 Tunable filter

A tunable receiver able to select various incoming channel signals in access networks is a key component for PON systems. Typical system architecture for TWDM PON using 4 wavelength laser transmitters and a tunable receiver is shown in the Figure 4:

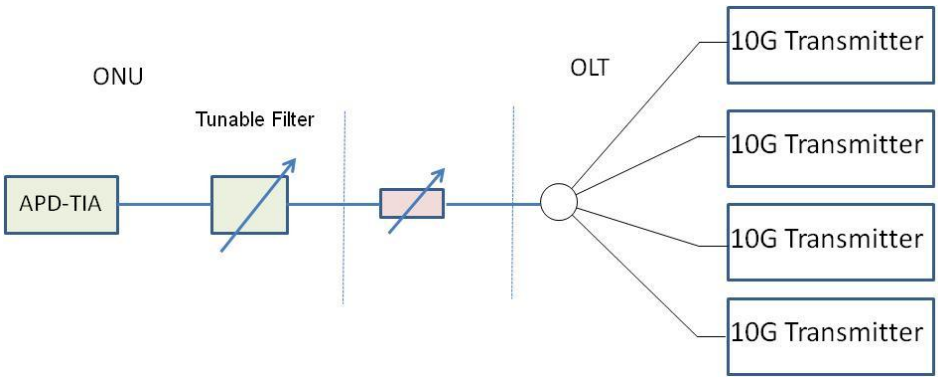

Figure 4 TWDM PON system architecture

Various technologies are foreseen for tunable filter fabrication. Indeed, a commercial product operating at a speed of 2.5Gbit/s is already proposed by Aegis (II-VI Incorporated) made of thin film filters and composed of amorphous Silicon and Silicon nitride layers [16]. Such kind of tunable filter (tunability is achieved through an integrated heater film) could be coupled to an APD to form the required tunable receiver. However, for higher bit rate applications (≥ 10Gbit/s), a small photodiode area is required to achieve a large bandwidth. As such, the optical coupling with the thin film tunable filter will be more complex leading to higher coupling loss which makes this solution less attractive for future generation PON systems.

A second solution to build an optical tunable filter is using bulk optic. Good performances can be achieved but at the expense of a large footprint. Integration with photodetectors is usually complex and might increase receiver cost. Typical performances achieved by bulk optic tunable filters are displayed in the Table 5:

Table 5 Typical performances achieved with bulk optic tunable filter

Parameter	Condition	Unit	Results
Wavelength range		nm	1525-1565
Free spectral range	1550 nm	GHz	465
Filter Pass-band width	@ 1dB	GHz	20
	@ 20dB	GHz	131
IL	1550 nm	dB	-1.61
Extinction ratio	± 100 GHz	dB	24
Tuning speed		ms	780
Working voltage		V	<4

Within DISCUS, our solution is based on Silicon Photonics which offers very small footprint and can lead to significant cost reduction owing to the maturity of Silicon technology processing.

We have already fabricated some tunable filters based on ring resonators, with integrated heaters.

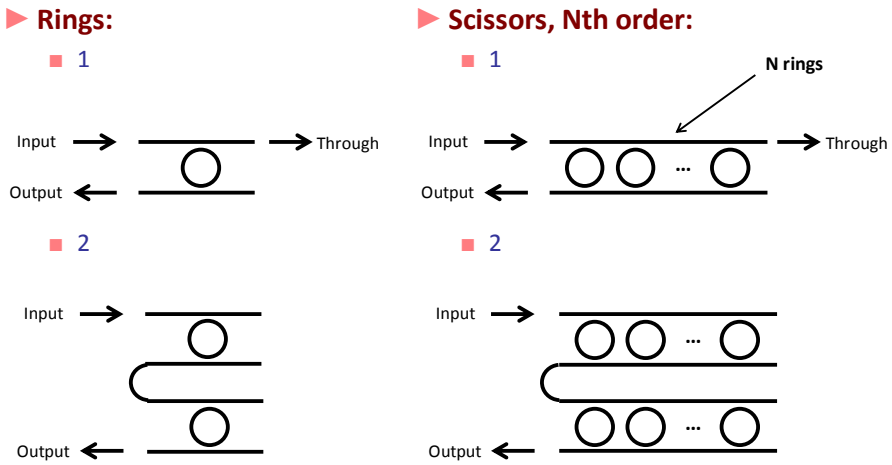

Figure 5 Possible configurations of the Si-based tunable filters. Scissor stands for Side Coupled Integrated Spaced Sequences of Optical Resonators.

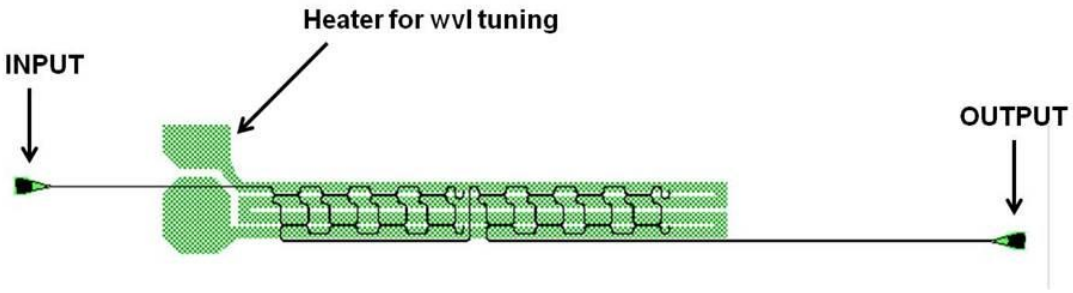

Figure 6 Practical implementation of a tunable filter with the integrated heater and the vertical couplers.

Figure 5 displays some configurations of the filters, which are based on serial and/or parallel integration of identical ring resonators. The size of the ring determines the free spectral range (FSR) of the filter. Typical FSR values are 1 to 20 nm. The coupling ratio between the straight waveguide and the ring influences the shape of the transmission curves. Figure 6 shows the heater implementation, which is distributed along the entire chip.

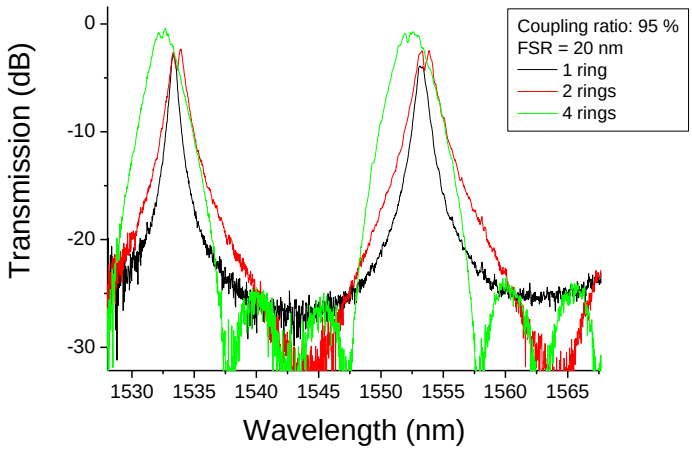

Figure 7: Transmission spectra of SCISSORS with 1, 2 or 4 parallel rings.

As can be seen on Figure 7, parallel integration of rings reduces the crosstalk, and increases the 1 dB bandwidth. Typical 1 dB bandwidth values are 50 to 100 GHz.

We have tested the wavelength tunability on the cascade of two Scissors made with 4 rings each.

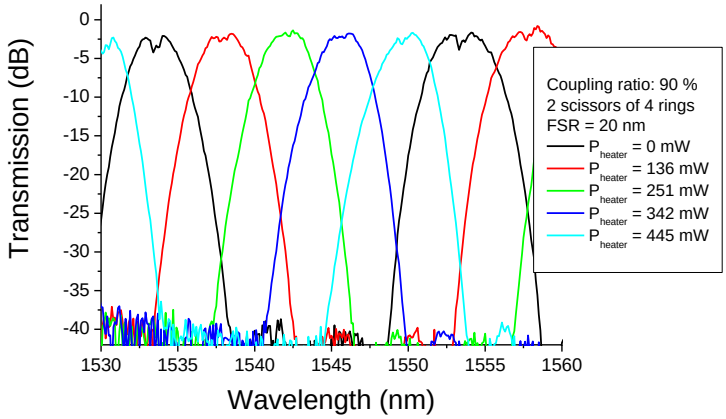

Figure 8: Transmission curves of 2 consecutive Scissors of 4 rings, as a function of the power dissipated by the heater.

Even with these un-optimized heaters, we have a tuning slope of 0.04 nm/mW.

In conclusion, Si-based filters display a large tunability and their 1 dB bandwidth can be easily controlled. However, the 20 dB bandwidth is too large with the existing designs (a few nm). Depending on the specifications on channel spacing and inter-channel crosstalk, we will have to optimize the design to meet the requirements.

Finally, we have measured the tuning speed of the filters, by modulating the heater current at 1 kHz between two wavelengths separated by 10 or 20 nm. For the latter case, we have kept the laser wavelength at 1.55 µm: the transmission of the filter at this wavelength became large once the filter had been tuned by 20 nm, which is the FSR of the rings we have studied here.

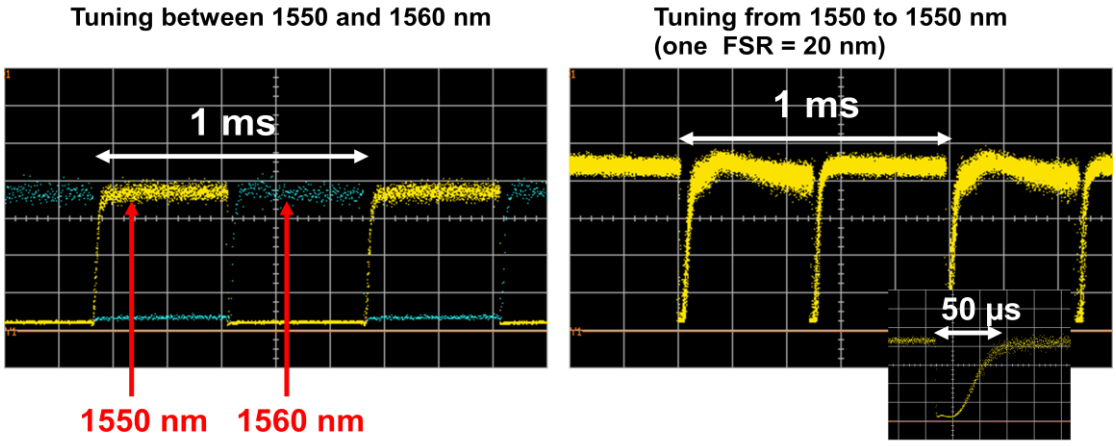

Figure 9: Transmission as a function of time when the filter is tuned by 10 nm (left) or 20 nm (right). Inset at the bottom right shows a tuning time of 50 µs when tuning the rings by 20 nm.

Figure 9 shows tuning times in the order of 50 µs when tuning the transmitted wavelength by 10 or even 20 nm with small rings, having a FSR of 20 nm. With larger rings (FSR = 4 nm), we have measured a tuning time of 100 µs typically.

There are some margins for improvement by changing the material separating the heater and the ring. Concerning the large rings, we can also reduce the heater surface.

2.4 Burst-mode electronic dispersion compensation

2.4.1 Need for burst-mode electronic dispersion compensation

The long reach (100km or beyond) of the hybrid DWDM/TDM LR-PON targeted in DISCUS in combination with a bitrate of 10Gbit/s necessitates the use of some form of chromatic dispersion compensation. This is especially true in the upstream direction of the network, where highly optimized transmitter technologies may be too costly. In previous hybrid DWDM/TDM LR-PON demonstrations, dispersion compensation was facilitated through the use of dispersion compensating fibre (DCF), which compensated for (a part of) the metro fibre link [6]. This is feasible as long as the fibre length of the access section is a small fraction of the overall length (for example a 90km metro section and a 10km access section). However from a network operator point-of-view, having the freedom to support much larger differential reaches (difference between maximum and minimum ONU-to-OLT fibre length), potentially as large as the total fibre length of the full LR-PON, can offer deployment advantages, especially in sparsely populated rural areas (see WP2).

In this case, it is no longer straightforward to compensate for the chromatic dispersion using a single length of DCF. Indeed, in principle one could use optical switches and a bank of different lengths of DCF, which are switched in the fibre link depending upon the fibre length between the central office and the ONU which transmitted the packet currently being received by the central office receiver. Such a solution however is expensive, bulky (physical space required for the different DCF modules and optical switches) and may have unacceptably large optical insertion losses.

A better solution is then to use 'burst-mode' electronic dispersion compensation (BM-EDC) [17], whereby the impairments originating from chromatic dispersion (and possibly other detrimental effects such as self-phase modulation) are compensated electronically (note that here we are assuming direct detection receivers, and hence have only access to the intensity of the incoming light). EDC is inherently adaptive, has negligible physical volume (ideally, the BM-EDC chip would replace the BM-CDR chip used in current PONs) and little capex and inventory cost compared to conventional DCF. Note that BM-EDC not just requires replacing the BM-CDR chip, but also requires a linear optical receiver: therefore in the upstream direction of the LR-PON it requires a linear burst-mode receiver (LBMRx). Such a device has been first demonstrated at Tyndall and will be discussed hereafter [18]. A second challenge is to make the EDC adaptive from burst to burst without requiring very large preambles at the start of each burst. Both aspects are discussed in detail hereafter.

2.4.2 *The linear burst-mode receiver*

A first requirement to implement BM-EDC is the availability of a LBMRx. From the system perspective, the following specifications/requirements are important:

- The required optical signal-to-noise ratio to achieve a given bit-error rate ($1.1x10^{-3}$ assuming forward error correction (FEC) based on Reed-Solomon RS(223,255), as widely used in 10G PON standards today);
- The required dynamic range, expressed as both the minimum (sensitivity) and maximum (overload) optical signal power that the LBMRx needs to be able to handle;
- The required linearity: according to accepted industry practice for linear optical receiver front-ends [19], this is expressed as total harmonic distortion (THD) for a sinusoidally varying input optical power. Typical numbers are less than 5% THD, a number comfortably achieved by the current LBMRx implementation [18].

Figure 10(a)+(b) summarizes the required optical signal-to-noise-ratio (OSNR) to achieve a BER of 1.1x10-3 at input dynamic ranges of 16dB and 20dB, as well as the burst-mode penalty (expressed as an OSNR penalty for a fixed input power) [20]. These numbers are currently used for dimensioning the optical distribution network of the DISCUS LR-PON.

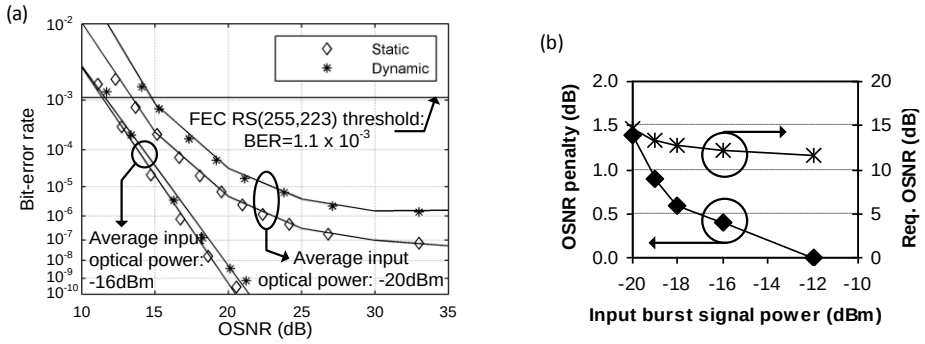

Figure 10(a) BER vs OSNR; Fig. 1(b) OSNR penalty due to preceding loud burst.

Next, it is important that the LBMRx can handle incoming bursts without requiring overly large guard times (the minimum allowable time between bursts, mainly required to reset the LBMRx after the end of a burst and prepare it for the next burst) and preambles (the data pattern at the start of the burst required for adjusting the gain and dc-offsets of the LBMRx). A good compromise between burst-mode penalty (the sensitivity or required OSNR (at a given BER) compared to the sensitivity or required OSNR of a conventional, continuous-mode receiver) and length of guard time and preamble is the following:

- Guard time: a guard time as short as 25.6ns can be supported by Tyndall's current LBMRx implementation;
- Preamble: the Tyndall LBMRx implementation requires ~50ns preamble length, which is well in line with e.g. existing 10G PON standards.

Additionally, following features allow more straightforward integration of the LBMRx into the complete receiver (including medium access control and LR-PON protocol) at the central office:

- Self-generation of a reset signal: this avoids the requirement of needing to know in advance the exact moment a burst arrive at the central office, which can be especially beneficial when the LR-PON is starting up for the first time (and the locations of the ONUs are unknown) or when new ONUs are attached to the network for the first time (when again the location of this ONU is not yet known);
- Indication of the start-of-burst: this is required for the subsequent BM-EDC chip, which will start its tap adaptation algorithm a fixed time (equal to the time required for LBMRx settling) after the indication of the start-of-burst.

2.4.3 High-level architectural considerations on the BM-EDC

Today, one can distinguish between three different approaches to implement electronic dispersion compensation:

1. *'Digital' approach*, in which the output of the optical receiver is digitized using a high-speed (at least two samples per bit) analog-to-digital converter (ADC) and recovered using digital signal processing (DSP). This approach allows implementation of highly sophisticated signal processing approaches such as maximum likelihood sequence estimation (MLSE), however at the expense of high complexity, power consumption and cost;
2. *'Mixed-signal' approach*, consisting of a cascade of a (symbol-spaced or fractionally-spaced) feedforward equalizer (FFE) and a decision feedback equalizer (DFE);
3. *'Analog' approach* consisting of a continuous time linear equalizer (CTLE), usually an amplifier with programmable zero(s) and pole(s).

For the DISCUS project, we have selected the 'mixed-signal' approach, as this gives the best trade-off between dispersion tolerance versus power consumption and complexity. Indeed while the 'digital' approach allows for implementation of e.g. MLSE, its ADCs and DSP are power hungry and expensive. Even though it is the least complex and requires smallest amount of power, the CTLE does not offer sufficient flexibility to set its frequency response to mitigate the chromatic dispersion.

2.4.4 Transmission performance of the mixed-signal approach

In a next step, it is important to investigate the transmission performance of the selected EDC method. To facilitate this, a simulation setup using VPI and Matlab software was used. For these initial results, an ideal (no chirp, infinite extinction ratio) transmitter was assumed. The receiver was modelled using a 4^{th} order Bessel-Thomson filter (3dB bandwidth: 8GHz). Figure 11 shows the transmission penalty vs. reach comparing the 'no EDC' case with an equalizer consisting of an 8-taps, T/2 spaced FFE and 2-taps DFE. It can be seen that for a 1dB transmission penalty, the equalizer extends the reach by ~60% to about 115km.

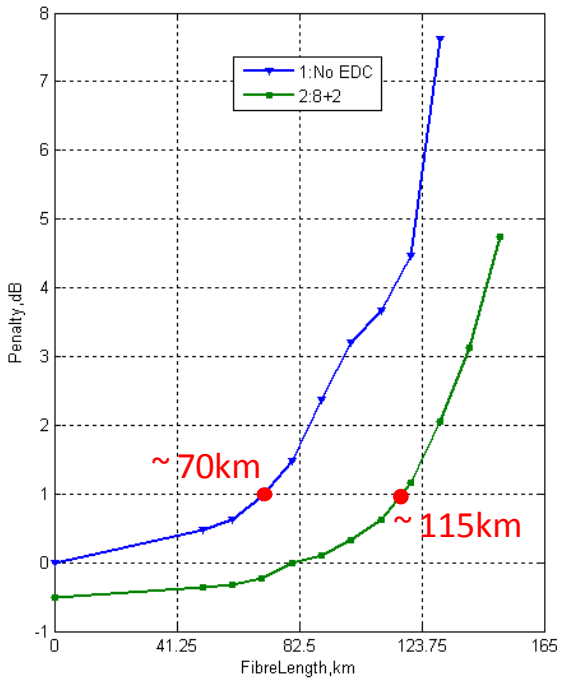

Figure 11 Extension of reach using an 8-taps FFE, 2-taps DFE.

An important trade-off when designing the EDC is the number of taps versus the improvement in transmission performance. A higher number of taps may improve the transmission performance, at the expense of a more complex and power-hungry BM-EDC chip. Figure 12 shows that beyond ~8 FFE taps, there is no appreciable improvement in transmission performance (reduction of transmission penalty). Even adding a single DFE tap helps significantly to improve the transmission performance, however no major improvement can be seen comparing the 1-tap and 2-tap DFE. These results suggest that a T/2, 8-taps FFE and 2-taps DFE could be an optimum choice for the considered LR-PON transmission scenario. This will be studied in more detail in WP5.

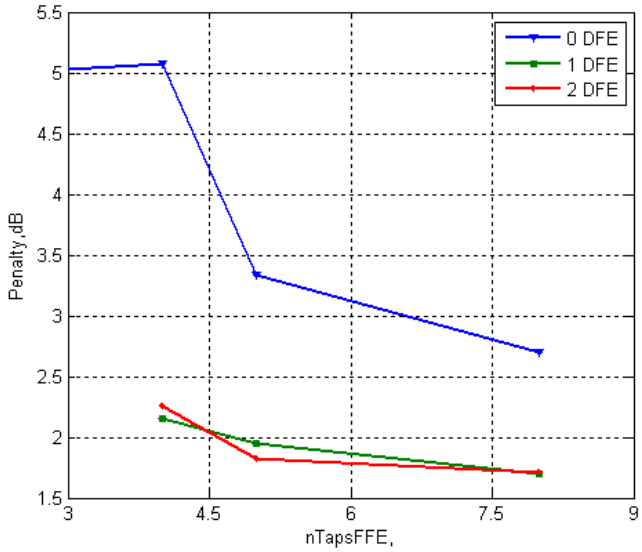

Figure 12 Transmission performance vs. number of taps in the T/2 spaced FFE, for different amount of DFE taps

2.4.5 Convergence of the tap adaptation algorithm

As the BM-EDC needs to adjust its tap settings from one burst to the next, an important consideration is the convergence speed of its tap adaptation algorithm. Figure 13 shows how the mean squared error between the EDC output and the ideal data sequence evolves as a function of the number of training bits used in the tap adaptation algorithm. These results were obtained for data sampled from an actual transmitter (based on a DFB laser externally modulated using an electro-absorption modulator and boosted using a semiconductor optical amplifier) using a real-time scope and post-processed using Matlab [17]. The assumed equalizer was a T/2 spaced, 9taps FFE and 3taps DFE, with 1400ps/km chromatic dispersion added. For the (relatively simple) case of the widely used least mean square (LMS) algorithm, tap adaptation within 500bits can be observed. When using the more complicated recursive least squares (RLS) algorithm, faster convergence within ~100bits can be observed. These results indicate that at least fundamentally it is possible to achieve convergence speeds (500bits at 10Gbit/s corresponds to 50ns) that are acceptable for PON applications. In a next step, it needs to be studied how to realize an implementation that does not require a large additional processing overhead. It is most likely that a variant of the signed-signed LMS algorithm will be implemented.

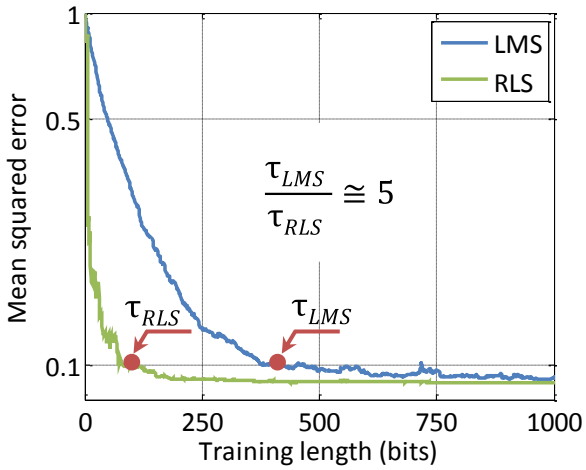

Figure 13 Convergence of the tap adaptation algorithm (LMS = Least Mean Squares algorithm, RLS = Recursive Least Squares algorithm).

2.4.6 Conclusion

Initial results on the system level aspects for a BM-EDC have been discussed. The requirements for a linear burst-mode receiver have been detailed; the choice for a 'mixed-signal' IC implementation for the BM-EDC has been weighed against the other major candidates and it has been shown that there are not fundamental show-stoppers that would prevent convergence of the BM-EDC taps in a time compatible with current PON standards.

2.5 Single carrier 40Gbit/s downstream upgrade scheme

The purpose of this section is to investigate and evaluate an upgrade path which is able to deliver a higher serial data rate (>10Gbit/s) in a LR-PON configuration. Speed upgrade from 10Gbit/s towards 40Gbit/s is challenging. There are several significant technical issues related to the speed increasing:

- The distortions which are induced by chromatic distortion (CD) grow with the square of the bit rate. For a given transmission distance, a 40Gbit/s system which has 4x increase in bit rate is 16 times more susceptible to CD than a 10 Gbit/s system.
- To maintain the receiver SNR when increasing the bit rate by a factor of 4 requires nominally 6 dB more optical power. While APDs have been used extensively in 10Gbit/s PON downstream to improve the receiver sensitivity, no high-speed APD devices are commercially available for 40Gbit/s NRZ operation.
- ONU electronics operating at the high line rate lead to further increase in power consumption. Considering the vast amount of subscribers, power consumption reduction in the ONU is of major importance.

For the 40Gbit/s downstream transmission a 3-level electrical duobinary modulation scheme is proposed to reduce the optical bandwidth of the OLT transmitter and ONU APD receivers. Duobinary modulation relaxes the downstream channel bandwidth requirement to ~20GHz thus improves the CD

tolerance significantly compared to the NRZ format. This allows for 25Gbit/s components (especially APDs) employed in ONUs, thus reducing the cost and power consumption.

CD was generally not an issue at 10Gbit/s rate for PONs. But it becomes a limiting factor when data rate further increases in combination with a longer reach. To extend the reach to 100km at 40Gbit/s the proposed scheme has to include a dispersion compensation element, such as a DCF or a fibre Bragg grating module at the OLT output. Because the DCF is shared between all users, it is not a cost-sensitive component. The extra insertion loss of DCF is of no issue as there is a downstream Erbium-doped fiber amplifiers (EDFA) right before the trunk fibre (assuming insertion of DCF does not deteriorate the OSNR significantly).

Moreover, to further decrease the ONU power consumption, we propose a 40Gbit/s bit-interleaving multiplexing PON (BiPON) scheme. Theoretically, the lower limit for the power-consumption in ONUs is dictated by the actual user-rate, which typically is a fraction of the aggregated PON line-rate. While conventional TDM-PON protocols are inherently operating at line-rate, the proposed bit-interleaving ONU (Bi-ONU) takes advantage of the line-rate – user-rate discrepancy. In every frame period, the Bi-ONU decimates and offsets the downstream payload. Because the decimation takes place on bit-level, the hardware afterwards is working at the user rate, significantly decreasing the power consumption.

2.5.1 OSNR requirements for 3-level duobinary modulation

To determine the theoretical OSNR requirements for 3-level duobinary modulation, we first assume a downstream signal with a large amount of optical noise which is much larger than the ONU receiver noise. In this case the dominant noise terms will be optical beat noise terms: signal-spontaneous and spontaneous-spontaneous beat noises. Therefore, the mean-square noise current at the receiver has two noise terms [21],

$$\overline{i_{n,ASE}^2} = \Re^2 \cdot (2P_S S_{ASE} + S_{ASE}^2 \cdot \Delta f) \cdot BW$$

where $\Re$ is reponsivity, P_S is signal power and S_{ASE} is optical noise density. Δf and BW are optical and electrical bandwidth respectively.

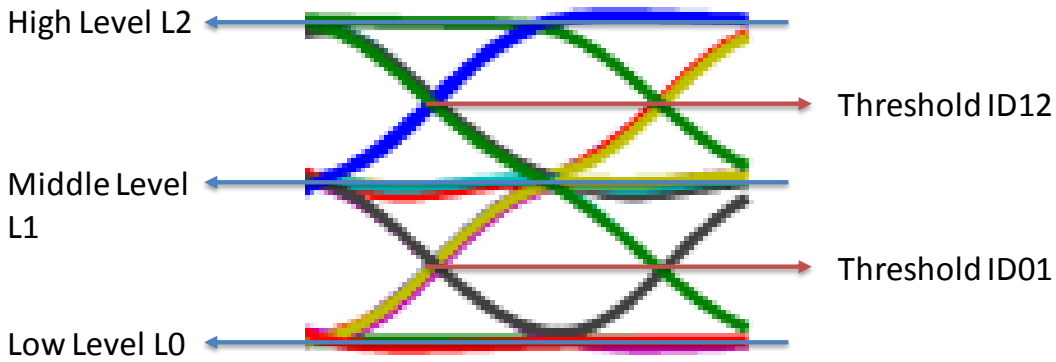

Figure 14 eye diagram and decision thresholds of 3-level duobinary signal

As illustrated in Figure 14, the electrical duobinary signal eye-diagram has 3 distinct levels, which present three transmitted symbols S_0, S_1, and S_2. If we define the extinction ratio as the ratio between high level power P_{S2} and low level power P_{S0}, i.e., $re = P_{S2}/P_{S0}$, we find the following relationship for finite extinction ratio re,

$$\overline{P_S} = P_{S1}$$

$$P_{S2} = \frac{2 \cdot re}{1+re} P_{S1}$$

$$P_{S0} = \frac{2}{1+re} P_{S1}$$

As expected, the noise current on three levels is different and can be found as,

$$\sigma_0^2 = \overline{i_{n,ASE,0}^2} = \Re^2 \cdot (2P_{S0}S_{ASE} + S_{ASE}^2 \cdot \Delta f) \cdot BW$$

$$\sigma_1^2 = \overline{i_{n,ASE,1}^2} = \Re^2 \cdot (2P_{S1}S_{ASE} + S_{ASE}^2 \cdot \Delta f) \cdot BW$$

$$\sigma_2^2 = \overline{i_{n,ASE,2}^2} = \Re^2 \cdot (2P_{S2}S_{ASE} + S_{ASE}^2 \cdot \Delta f) \cdot BW$$

where σ_0, σ_1 and σ_2 are the root-mean-square (rms) value of the noise currents.

At the receiver, an error will occur if at the sampling instant, the noise is greater than maximum allowed threshold level. We denote the error probability of receiving S_i when S_j was sent as,

$$P\{S_r = S_i \mid S_j\}$$

Note also that S_0 is sent with a probability of ¼, S_1 with a probability of ½ and S_2 with a probability of ¼. The overall error probability is given by,

$$BER = P_{e01} + P_{e12}$$
$$= \frac{1}{4}P\{S_r = S_1 \mid S_0\} + \frac{1}{2}P\{S_r = S_0 \mid S_1\} + \frac{1}{2}P\{S_r = S_2 \mid S_1\} + \frac{1}{4}P\{S_r = S_1 \mid S_2\}$$

where

$$P_{e01} = \frac{1}{4}P\{S_r = S_1 \mid S_0\} + \frac{1}{2}P\{S_r = S_0 \mid S_1\}$$
$$= \frac{1}{4} \cdot \frac{1}{2}\mathrm{erfc}\left(\frac{I_{D01} - I_{S0}}{\sigma_0\sqrt{2}}\right) + \frac{1}{2} \cdot \frac{1}{2}\mathrm{erfc}\left(\frac{I_{S1} - I_{D01}}{\sigma_1\sqrt{2}}\right)$$

$$P_{e12} = \frac{1}{2}P\{S_r = S_2 \mid S_1\} + \frac{1}{4}P\{S_r = S_1 \mid S_2\}$$
$$= \frac{1}{2} \cdot \frac{1}{2}\mathrm{erfc}\left(\frac{I_{S2} - I_{D12}}{\sigma_2\sqrt{2}}\right) + \frac{1}{4} \cdot \frac{1}{2}\mathrm{erfc}\left(\frac{I_{D12} - I_{S1}}{\sigma_1\sqrt{2}}\right)$$

From these equations, we can see that the BER depends on two decision thresholds I_{D01} and I_{D12}. In practice, both decision thresholds should be optimized to obtain the minimum BER. By setting

$$d(P_{e01})/dI_{D01} = 0,$$

we can solve the optimal threshold that minimizes P_{e01},

$$I_{D01,opt} = \frac{1}{\sigma_1^2 - \sigma_0^2}\left[\sigma_1^2 I_{S0} - \sigma_0^2 I_{S1} + \sqrt{\sigma_1^2\sigma_0^2(I_{S1}^2 + I_{S0}^2) - 2\sigma_1^2 I_{S1}\sigma_0^2 I_{S0} + 2\sigma_1^4 \ln\left(\frac{\sigma_1}{2\sigma_0}\right)\sigma_0^2 - 2\sigma_0^4 \ln\left(\frac{\sigma_1}{2\sigma_0}\right)\sigma_1^2}\right]$$

The second threshold $I_{D12,opt}$ can be calculated in a similar way.

Now with these equations in hand, we can estimate the required OSNR for a given BER threshold. For example, given an optical bandwidth of 12.5GHz (0.1nm bandwidth at λ = 1.55μm), an electrical bandwidth of 20GHz, extinction ratio of 12dB, the required OSNR is about 23.1dB for BER=1E-3. This is the case when the 3-level duobinary signal is generated by the downstream transmitter. Figure 15 shows the OSNR requirement versus extinction ratio for various BER thresholds with above assumptions.

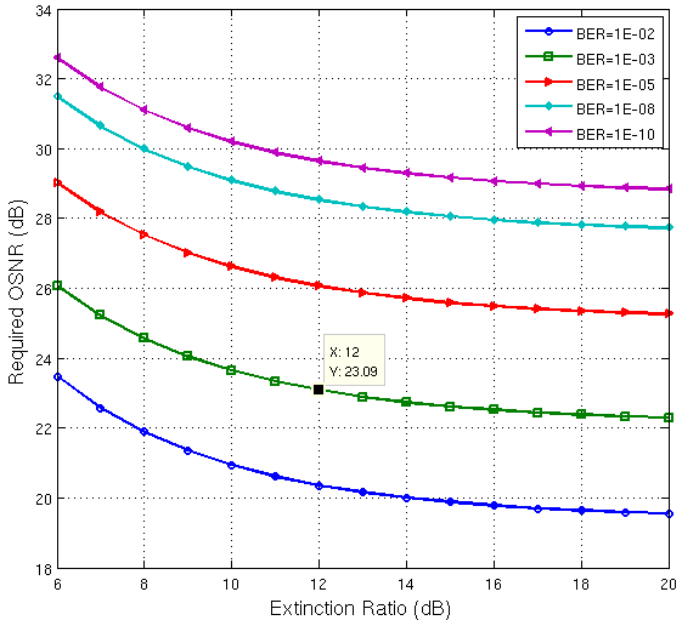

Figure 15 OSNR requirements in the back-to-back case versus extinction ratio when 3-level duobinary signal is generated at transmitter

Another way to generate 3-level duobinary signal is to utilise a low-pass filter with a bandwidth of ¼ data rate in the receiver [22]. This duobinary detection method allows for a 10GHz receiver at the ONU for 40Gbit/s downstream, and it requires a normal 40Gbit/s NRZ transmitter at OLT. Although the distortions caused by receiver bandwidth limitation will introduce extra power penalty, the smaller bandwidth reduces the OSNR requirement. For the same assumption but with a 10GHz electrical bandwidth, the required OSNR is about 20.1dB for BER=1E-3. Figure 16 shows the calculated OSNR versus extinction ratio when a bandwidth of ¼ data rate is used in the receiver.

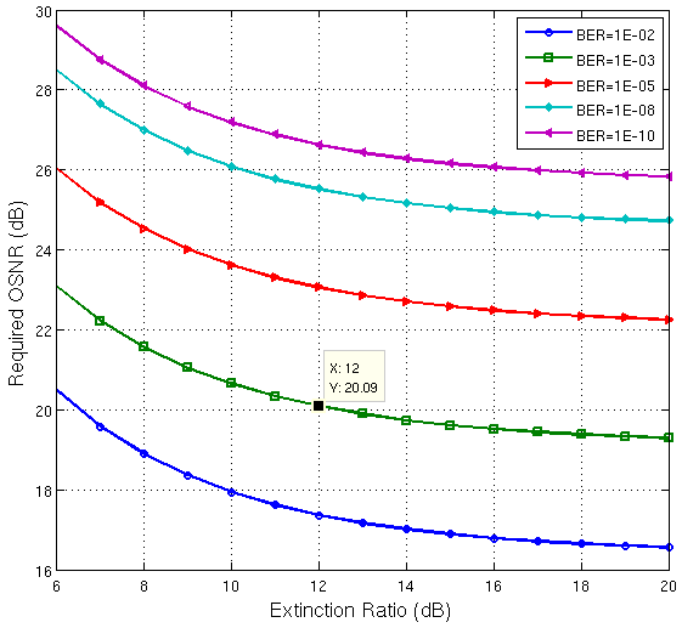

Figure 16 OSNR requirements in the back-to-back case versus extinction ratio when 3-level duobinary signal is generated at receiver

2.5.2 Power budget and OSNR modelling of 40Gbit/s downstream

- **Case 1: 40Gbit/s downstream using 3-level duobinary modulation and APD-Rx**

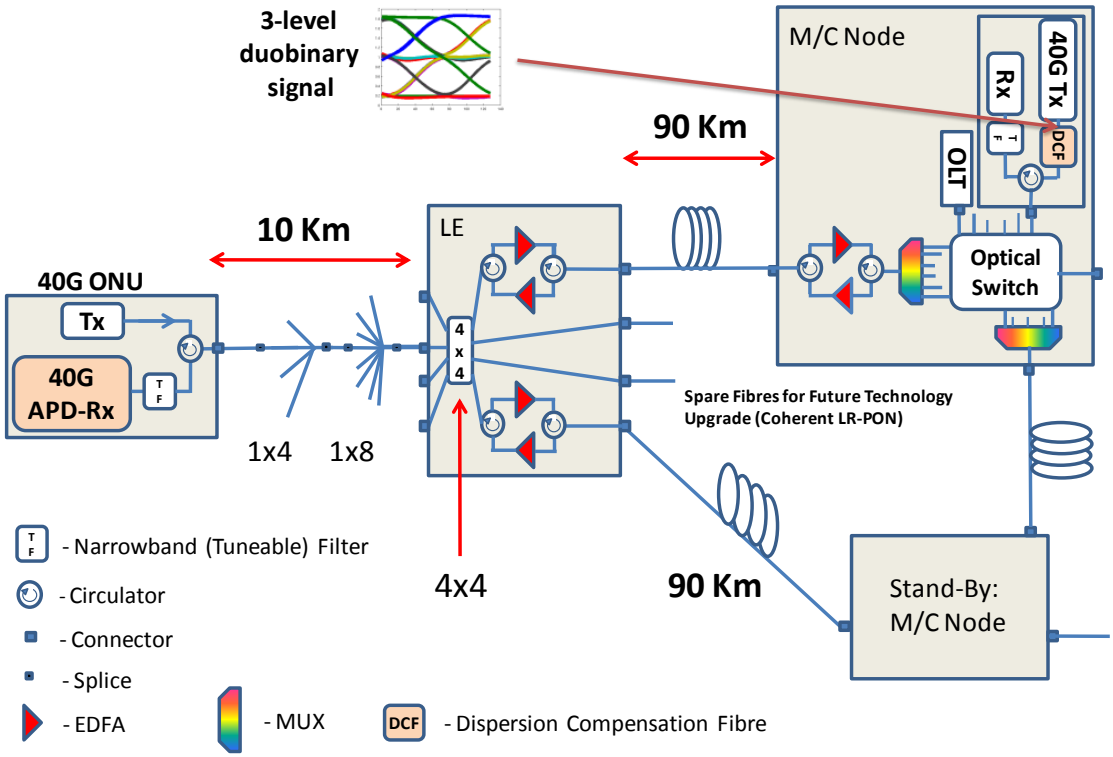

Figure 17 40Gbit/s downstream path with 3-level duobinary modulation.

Figure 17 shows the 40Gbit/s downstream topology with the 3-level duobinary modulation scheme. The losses of various components used in the modelling

have been summarised in Table 6. Given the optical power requirement of 40Gbit/s downstream, we assume a high power local exchange (LE) downstream EDFA with +17dBm output power and an EDFA in metro/core (MC) node with +10dBm output power. Both EDFAs have a noise figure of 5.5dB.

Table 6 Set of assumptions used for 40Gbit/s downstream power and OSNR modelling

	Min. Loss (dB)	Max. Loss (dB)	Noise Figure (dB)
DCF	5	5	0
Circulator	0.2	0.6	0
Connector	0	0.5	0
Fibre (per km)	0.2	0.3	0
Splice	0	0.3	0
1:2 Splitter	2.6	3.8	0
1:4 Splitter	5.4	7.1	0
1:8 Splitter	7.95	10.5	0
Mux/DeMUX	4	6	0
Optical Switch	1.8	2	0
Tuneable Filter	4	4	0
EDFA			5.5

Table 7 40Gbit/s downstream power and OSNR modelling with APD-Rx for 90km backhaul, 10km ODN and 128-way split

Components	Singal Power (Max) [dBm]	Noise Power (Max) [dBm]	OSNR (Max) [dB]	Singal Power (Min) [dBm]	Noise Power (Min) [dBm]	OSNR (Min) [dB]
40G Tx	9	-31	40	9	-31	40
DCF/TDC	5.0000	-35.0000	40.0000	5.0000	-35.0000	40.0000
Circulator	4.4000	-35.6000	40.0000	4.4000	-35.6000	40.0000
Connector	3.9000	-36.1000	40.0000	3.9000	-36.1000	40.0000
Optical Switch	1.9000	-38.1000	40.0000	1.9000	-38.1000	40.0000
Mux/Demux	-4.1000	-44.1000	40.0000	-4.1000	-44.1000	40.0000
Circulator	-4.7000	-44.7000	40.0000	-4.7000	-44.7000	40.0000
EDFA	10.0000	-29.3265	39.3265	10.0000	-29.3265	39.3265
Circulator	9.4000	-29.9265	39.3265	9.4000	-29.9265	39.3265
Connector	8.9000	-30.4265	39.3265	8.9000	-30.4265	39.3265
Fibre (90km)	-18.1000	-57.4265	39.3265	-18.1000	-57.4265	39.3265
Connector	-18.6000	-57.9265	39.3265	-18.6000	-57.9265	39.3265
Circulator	-19.2000	-58.5265	39.3265	-19.2000	-58.5265	39.3265
EDFA	17.0000	-15.2948	32.2948	17.0000	-15.2948	32.2948
Circulator	16.8000	-15.4948	32.2948	16.4000	-15.8948	32.2948
splitter1to4	11.4000	-20.8948	32.2948	9.3000	-22.9948	32.2948
Connector	11.4000	-20.8948	32.2948	8.8000	-23.4948	32.2948
splice	11.4000	-20.8948	32.2948	8.5000	-23.7948	32.2948
splitter1to8	3.4500	-28.8448	32.2948	-2.0000	-34.2948	32.2948
splice	3.4500	-28.8448	32.2948	-2.3000	-34.5948	32.2948
splice	3.4500	-28.8448	32.2948	-2.6000	-34.8948	32.2948
splitter1to4	-1.9500	-34.2448	32.2948	-9.7000	-41.9948	32.2948
splice	-1.9500	-34.2448	32.2948	-10.0000	-42.2948	32.2948
Fibre (0/10km)	-1.9500	-34.2448	32.2948	-13.0000	-45.2948	32.2948
Connector	-1.9500	-34.2448	32.2948	-13.5000	-45.7948	32.2948
Circulator	-2.1500	-34.4448	32.2948	-14.1000	-46.3948	32.2948
Tunable Filter	-6.1500	-38.4448	32.2948	-18.1000	-50.3948	32.2948

Here we assume a 25GHz APD receiver is used in 40Gbit/s ONU and a high power optical transmitter with +9dBm output power is used at the 40Gbit/s OLT. Table 7 shows the 40Gbit/s downstream analysis in terms of power and OSNR budget for a 90km backhaul, a 10km ODN and a 128-way split. Given the TX output power, the derived optical gains are 14.7dB and 36.2dB for the

downstream MC node EDFA and the LE DEFA respectively. As we do not have an optical pre-amplifier in the front of the downstream Rx the architecture will not be limited by the OSNR. This assumption is confirmed by the estimated OSNR (~32.3dB), which is sufficiently high for 40Gbit/s 3-level duobinary operation. Therefore, the relevant parameter is the input optical power. The minimum received signal power at APD input is -18.1dBm. The receiver needs a dynamic range of more than11.4dB to avoid overloading.

Since FEC is commonly employed in 10G-class PON systems to improve the optical link budget, we assumed a similar pre-FEC BER threshold of 10E-3 for the sensitivity estimation. We assume the APD receiver sensitivity for 40Gbit/s duobinary signal is -19.5dBm for BER=1E-3. Because of the bit-interleaving protocol, the downstream FEC decoder will work at much lower user rate, making more complex FEC codes feasible in ONUs. Therefore, if a strong FEC, such as low-density parity-check (LDPC) codes, would be used, it would give us some extra margin due to a higher pre-FEC BER [23].

This leads to the optical power margin shown in Table 8, assuming ~2dB sensitivity improvement by using a strong FEC.

Table 8 Optical power margin for 40G downstream with APD receiver

	Standard FEC (pre-FEC BER=1E-3)	Strong FEC (2dB improvement)
128 split	1.4	3.4
256 split	Negative margin	0

- **Case 2: 40Gbit/s downstream using pre-amplifier SOA in ONU**

In order to improve the optical budget, a semiconductor optical amplifier (SOA)-preamplifier with a PIN ONU receiver can be employed, as shown in Figure 18. The compact size and integrability of the SOA makes it a suitable candidate for the use as optical preamplifiers in ONU. But it usually has a higher inherent noise figure than EDFA. In the following power and OSNR analysis, an SOA with a noise figure of 7.5dB and maximum power gain of 12dB is assumed. As the gain of the SOA can be controlled by changing the bias current, the maximum gain assumption is applied here to lower the power consumption of ONUs. In the analysis, the real power gain of the SOA is derived on condition that the PIN-Rx is not overloaded (i.e., +3dBm at the input of the PIN-Rx). Other loss/noise figure assumptions are the same as shown in Table 6.

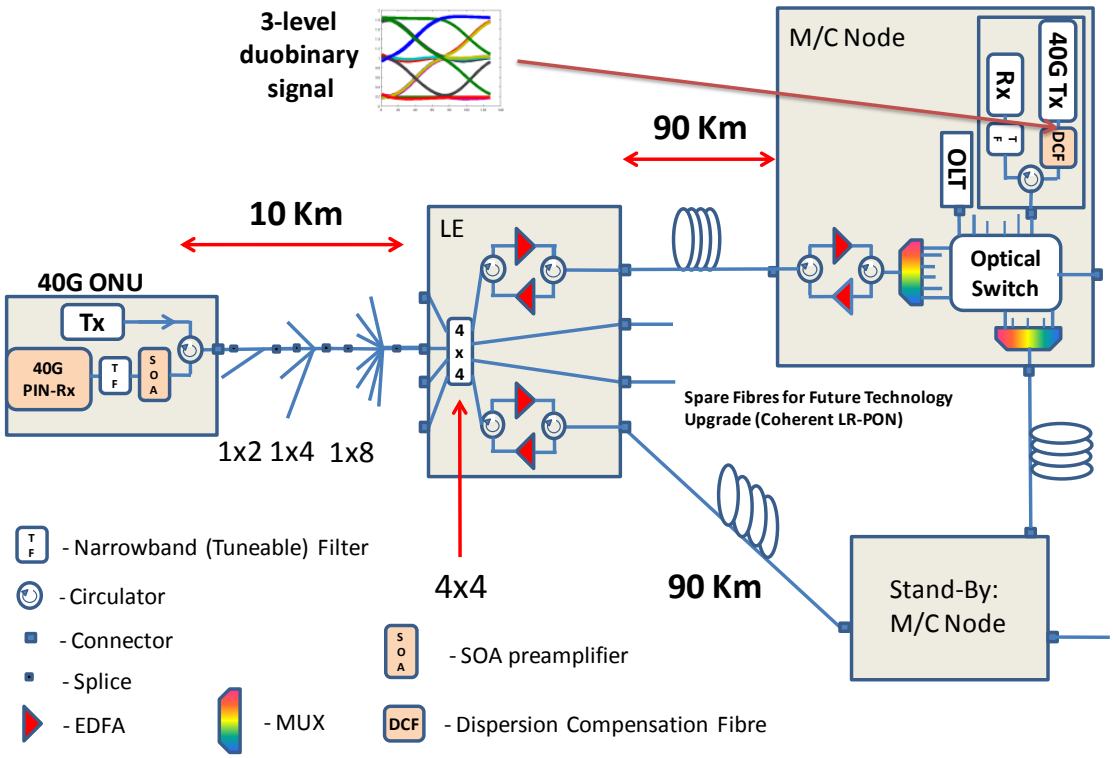

Figure 18 40Gbit/s downstream path with 3-level duobinary modulation

Table 9 shows the 40Gbit/s downstream analysis using a combination of an SOA and a PIN-Rx for a 90km backhaul, a 10km ODN and a 256-way split. Given the TX output power of +9dBm, the derived optical gains are 14.7dB and 36.2dB for the downstream MC node EDFA and the LE DEFA respectively. The gain of the ONU SOA is calculated as 11.3dB, which is smaller than the maximum optical gain assumption of 12dB. The power and OSNR results suggest that the downstream is still not limited by the OSNR (minimum 29.1dB) and the limitation comes from the receiver input optical power. In this case, the minimum received signal power at PIN-Rx input is -10.75dBm. The receiver needs a dynamic range of more than 13.75dB to avoid Rx overload.

Table 9 40G downstream power and OSNR modelling with SOA+PIN-Rx for 90km backhaul, 10km ODN and 256-way split

Components	Singal Power (Max) [dBm]	Noise Power (Max) [dBm]	OSNR (Max) [dB]	Singal Power (Min) [dBm]	Noise Power (Min) [dBm]	OSNR (Min) [dB]
40G Tx	9	-31	40	9	-31	40
DCF/TDC	5.0000	-35.0000	40.0000	5.0000	-35.0000	40.0000
Circulator	4.4000	-35.6000	40.0000	4.4000	-35.6000	40.0000
Connector	3.9000	-36.1000	40.0000	3.9000	-36.1000	40.0000
Optical Switch	1.9000	-38.1000	40.0000	1.9000	-38.1000	40.0000
Mux/Demux	-4.1000	-44.1000	40.0000	-4.1000	-44.1000	40.0000
Circulator	-4.7000	-44.7000	40.0000	-4.7000	-44.7000	40.0000
EDFA	10.0000	-29.3265	39.3265	10.0000	-29.3265	39.3265
Circulator	9.4000	-29.9265	39.3265	9.4000	-29.9265	39.3265
Connector	8.9000	-30.4265	39.3265	8.9000	-30.4265	39.3265
Fibre (90km)	-18.1000	-57.4265	39.3265	-18.1000	-57.4265	39.3265
Connector	-18.6000	-57.9265	39.3265	-18.6000	-57.9265	39.3265
Circulator	-19.2000	-58.5265	39.3265	-19.2000	-58.5265	39.3265
EDFA	17.0000	-15.2948	32.2948	17.0000	-15.2948	32.2948
Circulator	16.8000	-15.4948	32.2948	16.4000	-15.8948	32.2948
splitter1to4	11.4000	-20.8948	32.2948	9.3000	-22.9948	32.2948
Connector	11.4000	-20.8948	32.2948	8.8000	-23.4948	32.2948
splice	11.4000	-20.8948	32.2948	8.5000	-23.7948	32.2948
splitter1to8	3.4500	-28.8448	32.2948	-2.0000	-34.2948	32.2948
splice	3.4500	-28.8448	32.2948	-2.3000	-34.5948	32.2948
splice	3.4500	-28.8448	32.2948	-2.6000	-34.8948	32.2948
splitter1to4	-1.9500	-34.2448	32.2948	-9.7000	-41.9948	32.2948
splice	-1.9500	-34.2448	32.2948	-10.0000	-42.2948	32.2948
splice	-1.9500	-34.2448	32.2948	-10.3000	-42.5948	32.2948
splitter1to2	-4.5500	-36.8448	32.2948	-14.1000	-46.3948	32.2948
splice	-4.5500	-36.8448	32.2948	-14.4000	-46.6948	32.2948
Fibre (0/10km	-4.5500	-36.8448	32.2948	-17.4000	-49.6948	32.2948
Connector	-4.5500	-36.8448	32.2948	-17.9000	-50.1948	32.2948
Circulator	-4.7500	-37.0448	32.2948	-18.5000	-50.7948	32.2948
SOA	7.0000	-25.1011	32.1011	-6.7500	-35.8605	29.1105
Tunable Filter	3.0000	-29.1011	32.1011	-10.7500	-39.8605	29.1105

We assume the PIN receiver sensitivity for 40G duobinary signal is -12.5dBm for BER=1E-3. The resulting optical power margins are shown in Table 10, again assuming 2dB sensitivity improvement by using a strong FEC.

Table 10 Optical power margin for 40G downstream with SOA + PIN receiver

	Standard FEC (pre-FEC BER=1E-3)	Strong FEC (2dB improvement)
256 split	1.75	3.75
512 split	Negative margin	0.7

2.5.3 Dispersion penalty

One advantage of the 3-level duobinary modulation over NRZ modulation is its better chromatic dispersion tolerance. An experiment of a 26Gbit/s transmission over 40km has been demonstrated using duobinary detection at λ=1314nm [22]. To emulate this technology for DISCUS, the proposed 40Gbit/s downstream architecture has been simulated using a system simulator built with RSoft Optsim and Matlab. Because we will include a dispersion compensation module at the output of the OLT to compensate the common optical path, i.e. backhaul, the maximum differential reach is 10km in the access section. The simulated eye-diagrams of 40Gbit/s NRZ for 0, 2km, 4km, 6km, 8km, and 10km reaches are shown in Figure 19. It can be noted that the NRZ eyes are getting really closed after reach of 6km. As a comparison, the eye-diagrams of 40Gbit/s 3-level duobinary signal for 0, 2km, 4km, 6km, 8km, and 10km reaches are shown in Figure 20. Even at 10km reach, a 3-level signal is still able to be recognized from the eye-diagram.

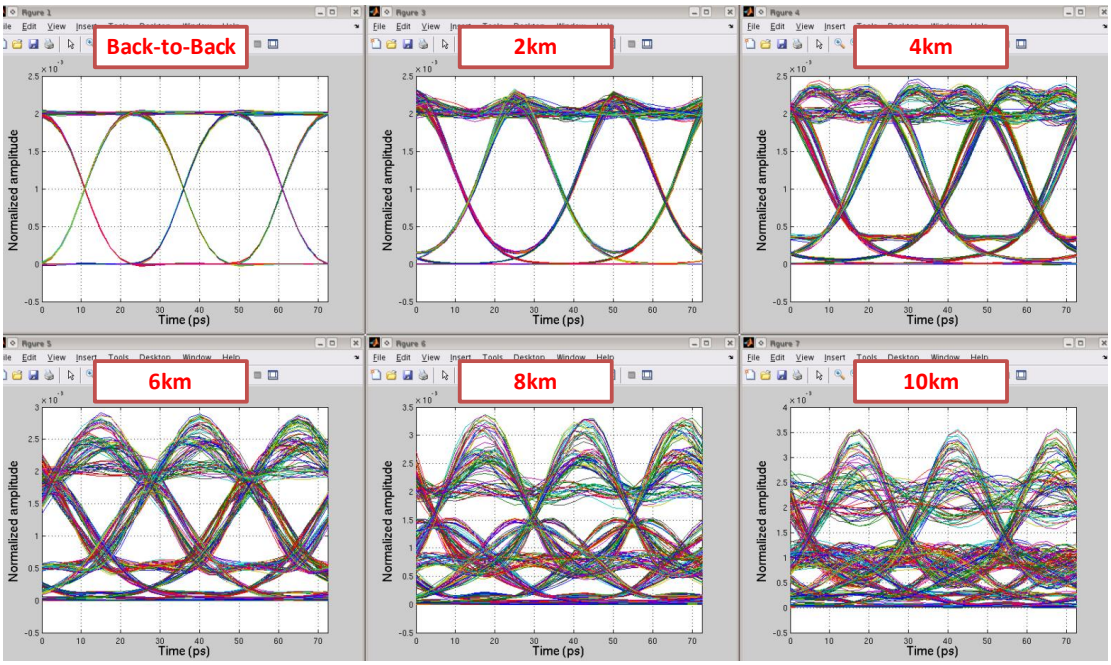

Figure 19 Eye-diagram of 40Gbit/s NRZ for various reaches

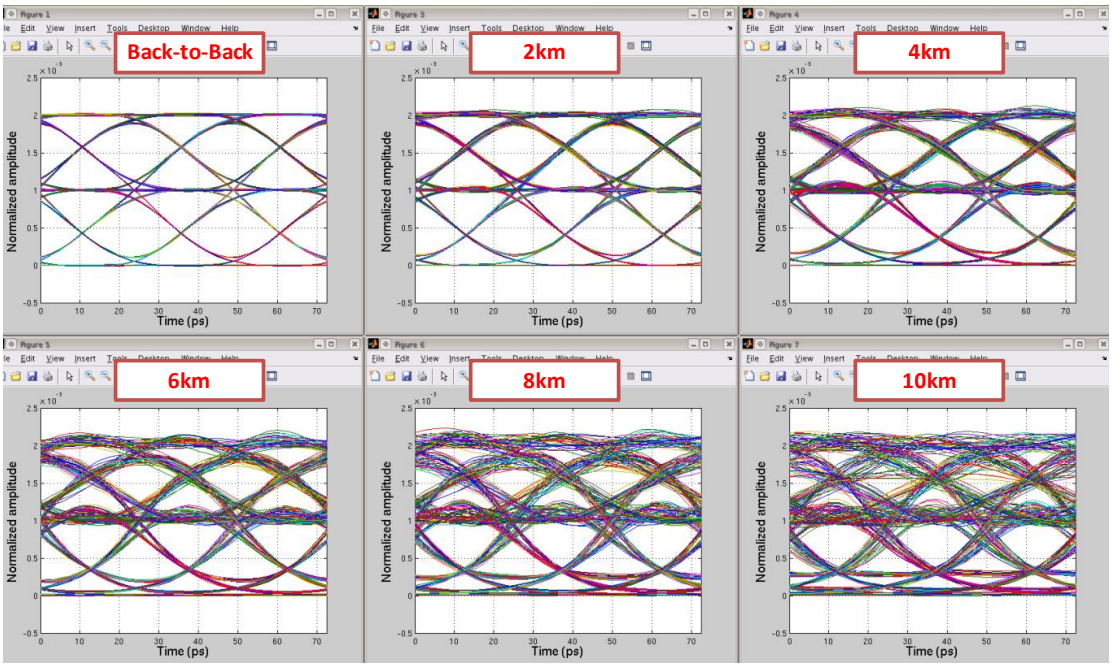

Figure 20 Eye-diagram of 40Gbit/s 3-level duobinary signal for various reaches

In order to illustrate the benefit of choosing 3-level duobinary modulation, we have simulated the impact of chromatic dispersion using Monte-Carlo techniques. Specifically, we have run simulations of both 40Gbit/s NRZ and 3-level duobinary system for different fibre lengths and observed the power penalties with respect to their back-to-back cases. We assumed APD receivers used and a pre-FEC BER threshold of 1E-3 for sensitivity penalty calculations. The resulting power penalties for these two modulation formats are listed in Table 11. For the 40Gbit/s NRZ signal, it cannot meet pre-FEC of 1E-3 when the transmission length is higher than 6km. Furthermore, at transmission length of 6km, the

power penalty of 40Gbit/s 3-level duobinary transmission is much smaller than that of 40G NRZ signal (1.3dB versus 3.1dB).

Table 11 Optical power penalties versus fibre lengths for 40G NRZ and 3-level duobinary modulation

Distance (km)	Dispersion Power Penalty (dB)	
	40G NRZ APD-Rx	40G 3-level duobinary APD-Rx
2	0.1	0.1
4	0.5	0.6
6	3.1	1.3
8	Does not work	2.6
10	Does not work	5.8

Given a differential reach of 10km, the nominal dispersion length should be chosen as the mean of the distance of the shortest and the longest reach. For the 40Gbit/s architecture discussed so far, the shortest reach is 90km and the longest is 100km. Thus the dispersion compensation element should compensate about 95km of fibre, which leaves uncompensated length of ±5km. In the following analysis, we will assume that system margin should be larger than the dispersion power penalty for 6km reach (i.e., 5km+1km extra margin assumed).

Similar simulation has been done for the SOA-PIN receiver using 3-level duobinary modulation, assuming optical noise is negligible. At distance of 6km, the dispersion penalty is about 0.9dB instead of 1.3dB for the APD receiver.

Taking the power margins shown in Table 8 and Table 10, the dispersion penalties at 6km for both the APD and the SOA-PIN receivers should be subtracted to evaluate the final system margin. Therefore a 40Gbit/s APD receiver using 3-level duobinary almost cannot support 100km reach and 128-split (only 0.1dB margin). If we use a strong FEC, assuming 2dB sensitivity improvement, the power margin would be 2.1dB. On the other hand, the SOA-PIN receiver can be used in the ONU to achieve a split ratio up to 256; it gives a margin of 0.85dB with a standard FEC and 2.85dB with a strong FEC respectively.

2.5.4 Conclusion

As part of the evolutionary strategy, 40Gbit/s transmission in the downstream direction is investigated as an upgrade option. To upgrade to a single-carrier 40Gbit/s downstream in LR-PONs, a 3-level duobinary modulation scheme with downstream BiPON protocol is proposed. The 3-level duobinary relaxes the component bandwidth requirement at ONU and shows better tolerance for chromatic dispersion. The BiPON protocol would further reduce the power consumption and enable cost-effective implementation of advanced FEC codes because the FEC decoder only needs to operate at the user rate. The 40Gbit/s downstream topologies with APD and SOA-PIN receivers have been analysed in terms of power and OSNR budget. Assuming a strong FEC with 2dB power budget improvement, an APD receiver would support a 90km backhaul, a 10km ODN and a 128-way split while a SOA-PIN receiver would allow for an upgraded split ratio of 256 at 40Gbit/s.

3 Coherent Detection Scheme (WDM LR-PON)

Coherent optical communication has been well established as the technology of choice for long haul and high bit rate communication systems since mid 2000. Recent technology evolution and ongoing price erosion further open the window of opportunity for the application of coherent optical transmission technology in other domains. This chapter gives an overview of the capabilities, design and implementation of a coherent ultra dense WDM technology for optical metro and access networks. Its capabilities enable a number of attractive options, such as a wide range of downstream bit rates from 150 Mbit/s up to 10 Gbit/s per user, and the coexistence with existing systems such as GPON, EPON, XGPON or RF-Video in existing optical distribution networks. Due to its flexibility and capacity, it is also suitable for deployments in metropolitan networks, as well as for mobile front-haul and back-haul networks.

3.1 System design and capabilities

An example of a basic coherent UDWDM network design is given in Figure 21. An OLT generates up to 1000 wavelengths in an ultra-dense wavelength grid. The specific wavelength spacing, typically at 3 GHz, will be explained in Section 3.3. All wavelengths are transmitted on the same standard single mode fiber (SSMF). The light on that fiber is then distributed equally to all branches of the PON tree if there are only wavelength agnostic passive splitters in the distribution network (ODN) as shown in the upper path of Figure 21. It is also possible to use wavelength filters, such as arrayed waveguide gratings (AWGs), in the distribution node in order to select specific wavelength bands (Figure 1, lower path). The optical insertion loss of AWGs is lower than that of passive splitters for split factors higher than 8, so AWGs can be used to decrease the optical path loss of the ODN, thus increasing the reach distance. When an AWG is used in the ODN, not all wavelength are routed to all users, potential privacy issues are better addressed. On the other hand, AWGs in the ODN can reduce the flexibility of the whole system and do not allow flexible re-assignment of wavelengths.

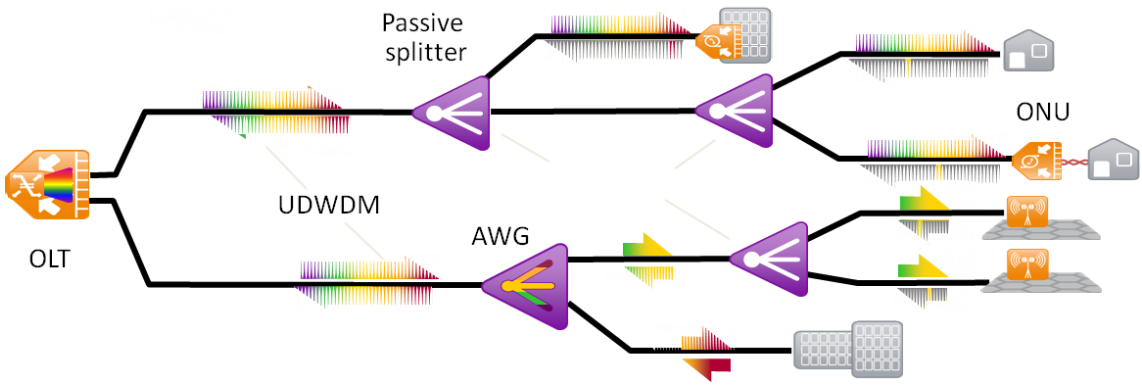

Figure 21: Basic system design

Depending on the ODN configuration, each user receives all wavelengths or a subset thereof. The intrinsic wavelength selectivity of coherent reception allows the ONU to detect only the intended wavelength and ignore all other wavelengths. Each ONU is fully tunable in the C-band. Each wavelength carries 1 Gbit/s payload. Data rate per user can be selected between 150 Mbit/s and 10 Gbit/s based on the technique described in more detail in Section 3.9. Privacy is ensured by encryption at the data layer. The high sensitivity of coherent reception allows for an optical loss budget of 43 dB which can be traded arbitrarily for reach and split. Depending on the ODN configuration, the power budget allows the connection of up to 1000 users with a reach of up to 100 km, however with a pure passive splitter, both extremes cannot be achieved at the same time.

3.2 Basic working principle: Paired Channel Technology

The high number of closely spaced wavelengths prohibits the use of external wavelength locking components in the ONU for upstream wavelengths, as the needed ultra-high precision and stability of such wavelength lockers prevent an economical implementation. An innovative implementation called "Paired Channel Technology" (PCT) is introduced as a practical and economical way to generate very closely spaced wavelengths without the use of wavelength lockers. The key idea of the PCT is to lock the ONU upstream wavelength to the received downstream wavelength as shown in Figure 22. The detection and locking of the downstream wavelength relies on coherent reception by use of a tunable local oscillator (LO) laser in the ONU. The combined requirements of a LO laser and a locking mechanism make re-using the LO laser for upstream the natural choice. Part of the LO laser light is directly modulated and used as the upstream signal. Note that a system which uses the exact same wavelength for the upstream as the downstream in a single fiber configuration would be very sensitive to back reflections from the ODN. To minimize the effect of back reflections, the upstream wavelength is detuned from the downstream wavelength by +933 MHz.

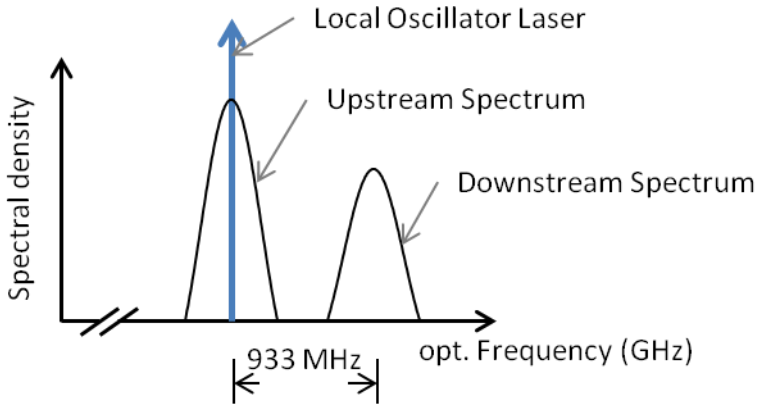

Figure 22: Spectral position of the downstream and the upstream wavelength in the ONU

On the OLT side, it would be highly impractical and expensive to use 1000 lasers which are all locked to the respective, ultra fine grid. Therefore, the practical solution is to generate multiple wavelengths out of a single laser source that also serves as a local oscillator for the coherent reception of the

corresponding upstream wavelengths. Such a unit, generating and receiving 10 wavelengths, is called Optical Transceiver Group (OTG). Figure 23 (a) shows the spectral position of the downstream wavelengths of an OTG, the corresponding upstream wavelengths, and the respective back reflections. The frequency is scaled in units of =933 MHz. The two downstream wavelengths with the smallest frequency deviation from the originating carriers have a spectral distance from the carrier of 2 Δ =1866 MHz (resulting in a total distance of 4Δ) while all other carriers have a spectral distance of 3 Δ =2799 MHz.

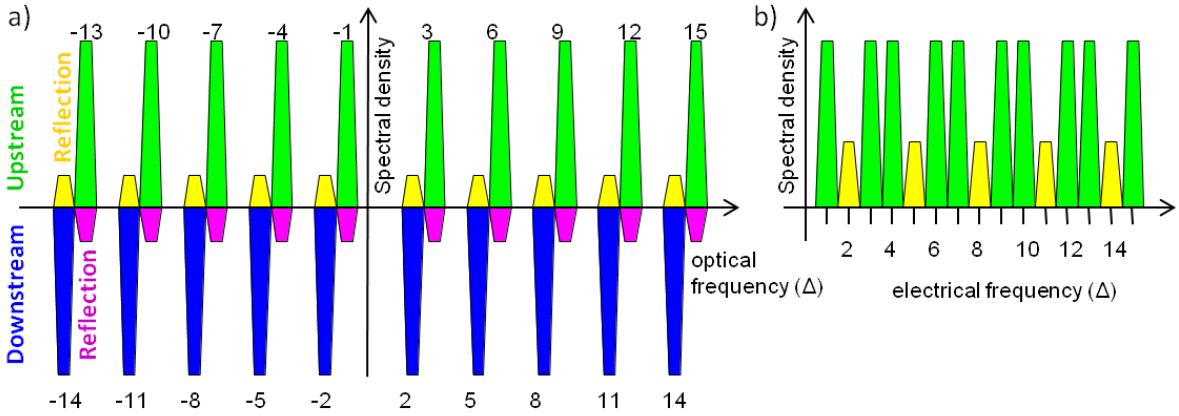

Figure 23 a) wavelength scheme of one Optical Transceiver Group, Transmit direction. b) electrical spectrum at the OLT receiver. All frequencies are denoted as multiples of Δf=933 MHz

The reason for this specific wavelength spacing design can be seen in Figure 23 (b) which is the electrical spectrum of the wavelength map in Figure 23 (a). The laser at the central carrier frequency serves as local oscillator for the OLT reception. The upstream wavelengths are superimposed with this laser and detected by a balanced pair of photodiodes. As the ONUs lock on to the downstream wavelength, the symmetric downstream spectrum (Figure 23) is converted to a spectrum in the OLT receiver where each upstream wavelength falls into a specific frequency range (green bars in Figure 23). The back reflections, on the other hand, add up in the 'garbage' frequency bands of {2, 5, 8, 11, 14}*933 MHz.

Figure 24 (a) shows as an example the simulated electrical spectrum after the OLT receiver. In this specific case, the back reflections have higher amplitude than the payload signal, but due to the pulse shaping (see Section 3. 4) and the resulting spectral separation relatively high back reflection levels can be tolerated. Figure 24 (b) shows the dependence of the necessary OLT Rx power for different BERs. It can be seen that for a BER of 10-6 and an OLT Rx input power of -40 dBm, about -24 dB of back reflection can be tolerated. A detailed analysis of the back reflection topic can be found in [24].

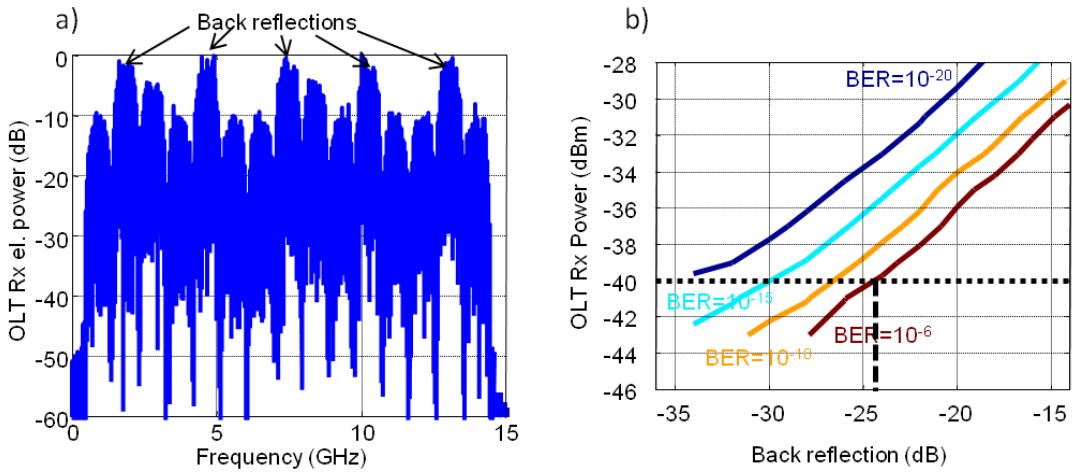

Figure 24: a) simulated OLT Rx electrical spectrum, b) simulated BER vs. back reflection level

3.3 Clocks, Frequencies and Frequency relations

The frequencies in the system are selected to make data processing as efficient as possible. To this end, all clocks and frequencies in the system, including the wavelength spacing, are integer multiples of a base frequency. This base frequency is chosen to be STM 1 at 155.52 MHz, and the factors are either powers of 2 or three times powers of 2.

The data rate of 1244.16 MHz is 8 times the base frequency (e.g. STM 8) . As DQPSK with two bits per symbol is used as modulation format, the symbol rate is 622.08 MHz. The base unit for the wavelength spacing is six times the STM 1 rate, e.g. 933.12 MHz. Such a frequency slot can host a 622.08 Mbaud signal with a square root raised cosine pulse shaping (roll off=0.5) and leaves some room for laser drifts.

In the OLT transmit direction, the high speed digital to analog converters run at 57.71968 GSamples/s which equals 384 times the STM 1 frequency or 64 times the wavelength spacing Δf.

The ONU receiver analog to digital converters (ADC) sample at 3.73248 GSamples/s which equal 24 times the STM 1 rate. As heterodyne reception with an intermediate frequency of 933.12 MHz is used (see later sections), the ADC sampling rate equals four times the intermediate frequency. This enables efficient digital downconversion algorithms.

3.4 Bit rate flexibility

The system offers a wide span of sustained bit rates for the user. Bit rates lower than 1.244 Gbit/s are realized by sharing one downstream wavelength among up to 6 ONUs in a Time Domain Multiplexed (TDM) manner. The upstream direction remains as WDMA. The available upstream spectrum is shared by up to 6 ONUs. By doing so, the disadvantages of a TDM upstream scheme, e.g. burst mode, time slot allocation protocols and related issues can be avoided. This is sketched in Figure 25. Each of the upstream spectral bands represents a different ONU. As

the LO lasers are not optically phase locked, guard bands are needed in between the ONU signals in order to avoid crosstalk. In short, up to 6 ONUs share a downstream wavelength by TDM means (in downstream, TDM adds no significant penalty) and in upstream each of the ONUs still has its own WDM wavelengths within the spectral window of the else used 1.244 Gbit/s upstream. In total, up to 60 ONUs can be connected to one single OTG.

For coherent transmission systems, the dependence of the possible symbol rate and the modulation format from required laser linewidth has been shown in numerous publications [30]. The restricted upstream spectra per ONU (about 70 MHz) operating at lower bit rates would require a laser linewidth on the order of a few 10 kHz to transmit QDPSK modulated data. Such a small laser linewidth is challenging in a cost sensitive system. In order to be able to use the same 500 kHz linewidth laser, the modulation format is changed to On-Off Keying (OOK), resulting in an upstream data rate of 69 Mbit/s per ONU.

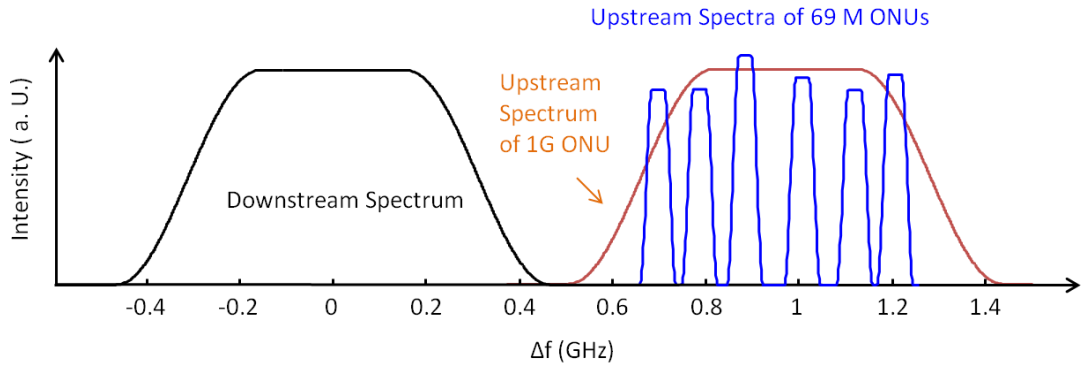

Figure 25: **Upstream wavelength assignment for the multiple ONUs per wavelength case**

As the ONU uses an upstream IQ-Modulator, the generation of the upstream light is software defined and the same physical hardware ONU can either generate a 1.244 Gbit/s upstream, or one or more 69 Mbit/s upstreams, modulated with On Off Keying.

Bit rates of for example. 5 or 10 Gbit/s are realized by combining the wavelengths transmitted by one OTG and using a second OTG as an ONU. A 10 Gbit/s ONU thus uses the same hardware as an OTG in the OLT, and receives and transmits 10 wavelengths each at 1.244 Gbit/s simultaneously.

3.5 Real Time OLT

The block diagram of a real time UDWDM OLT is shown in Figure 26. In this implementation, one single laser is needed to generate 10 wavelengths. An FPGA performs the baseband processing to generate 1.244 Gbit/s data streams out of a 1 Gbit/s Ethernet signal for each of the 10 wavelengths. The FPGA also performs framing, forward error correction (FEC) encoding, and functions such as differential encoding and scrambling of the bit streams. The 10 resulting bit streams, each at 1.244 Gbit/s, are then transferred into an ASIC, which consists of 10 parallel up-conversion, pulse shaping blocks, and a pair of digital to analog converters (DACs). The up-converters transfer baseband data onto high frequency, DQPSK modulated carriers. The carrier frequencies are integer

multiples of a base frequency grid of 933 MHz. The carrier frequencies are {-14, -11, -8, -5, -2, 2, 5, 8, 11, 14}*933 MHz. In the ASIC, the high frequency carriers are represented as 8-bit data streams for both the In-Phase ('I') and the Quadrature ('Q') components. In order to have a clear separation of the wavelengths, a square root raised cosine pulse shaping filter (roll-off factor=0.5) is applied. The I and Q components of all high frequency carriers are then added and converted into electrical currents by two high speed DACs at a sampling rate of 59.7 GSamples/s.

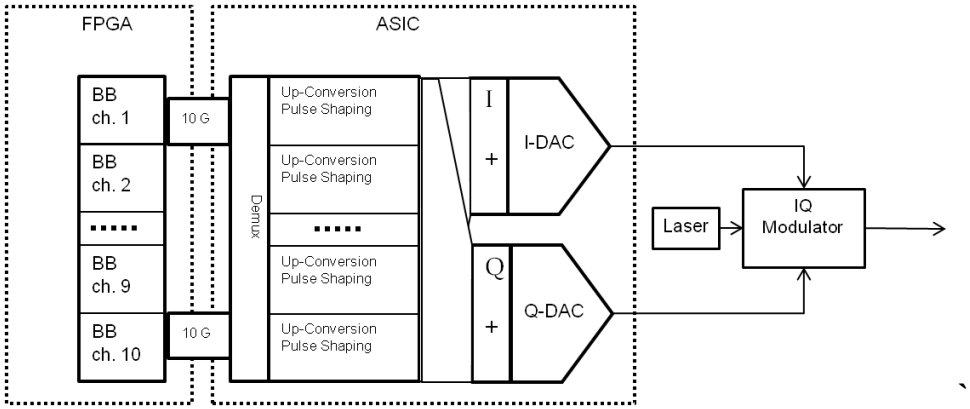

Figure 26: **OLT transmit path block diagram**

The two output currents from the high speed DACs are then amplified and used to drive an IQ-modulator which modulates the light from a narrow linewidth laser. The IQ modulator is operated such that it generates single sideband signals. Each of the 10 electrical channels generates its own single sideband signal so that each resulting wavelength is individually modulated with a pulse shaped 622 Mbaud DQPSK signal. Figure 27 depicts the generated spectra.

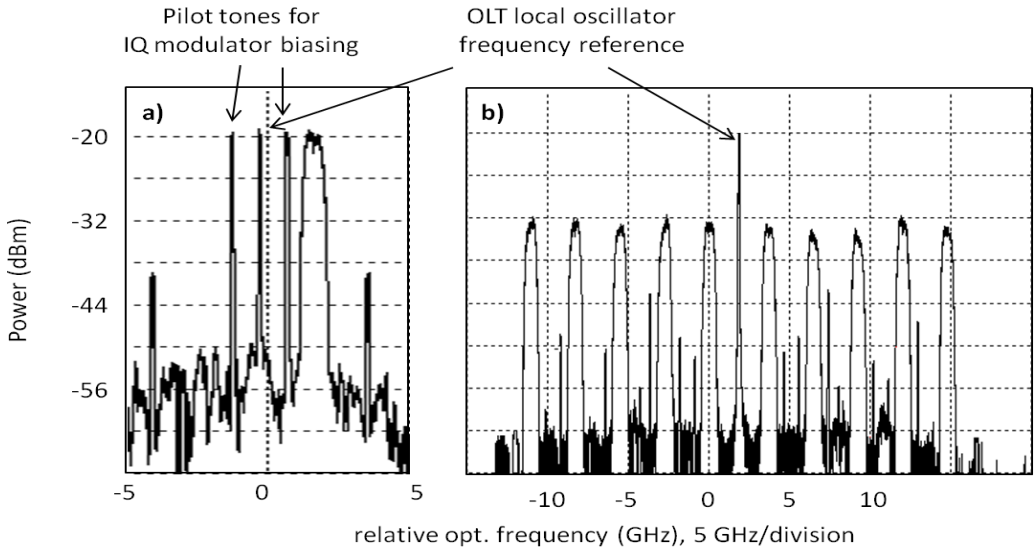

Figure 27: **output spectra of the OLT transmit block. a) one active wavelength, b) 10 active wavelengths.**

In order to demonstrate and verify the single sideband operation, only one carrier is active in Figure 27(a). It can be seen that the sidebands are suppressed by about 30 dB. The residual carrier is visible as well as two pilot tone lines at ±933 MHz which serve for the adjustment of the right biasing of the IQ modulator. In Figure 27(b) all 10 wavelengths were activated. The narrow, small spectral lines which can be seen close to the payload wavelengths are generated by residual clock spurs of the DAC. They carry negligible energy and do not cause a negative effect on the system performance.

Practical implementations of coherent receivers have been described extensively and will not be repeated here. A good overview can be found in [25] and references therein. In [26], some details about the phase estimation are described. On the receive side of the OLT, a wideband polarization diverse coherent receiver is used. The same laser which generates the 10 downstream wavelengths is used as a local oscillator for the reception of the 10 upstream wavelengths. A pair of 60 GSamples/s ADCs digitizes the signals. The data streams are then filtered and down-converted in parallel by a Weighted OverLay and Add (WOLA) structure [27],[28] and received by a bank of 10 parallel 1.244 Gbit/s DQPSK decoders, un-framers and FEC units.

3.6 Real Time ONU

The ONU consists of an integrated optical module, a FPGA, and a set of ADC/DAC as interfaces between the optical module and the FPGA.

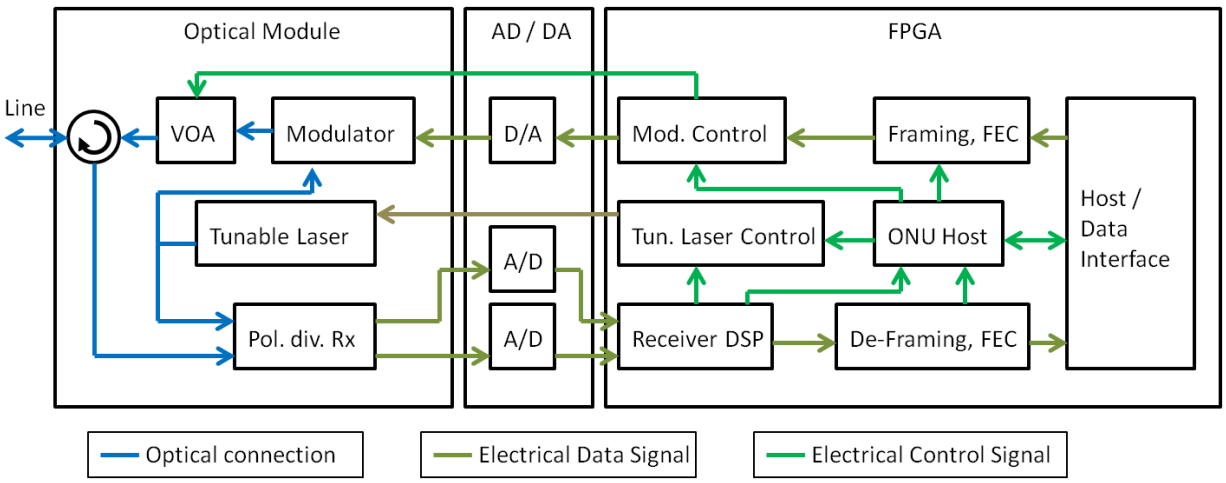

Figure 28: Block diagram of the ONU

As shown in Figure 28, the optical module (more details in [29]) consists of a tunable laser, a polarization diversity receiver, an IQ modulator, and a Variable Optical Attenuator (VOA) as upstream transmit power control. The tunable laser covers the full C band and has a linewidth of below 500 kHz. The polarization diversity receiver is configured as a heterodyne receiver with a heterodyne frequency of about 1 GHz and is equipped with linear low noise transimpedance

amplifiers. The IQ modulator performs the DQPSK modulation. A SOA serves as a VOA as well as a transmit power booster in order to either switch off the upstream light when the ONU is scanning (see Sec. 3.7) or to set the right level of upstream transmission mode.

The output signals from the polarization diversity receiver are amplified and digitized by a pair of 3.8 GSamples/s, 8 bit ADCs and then fed into the FPGA receiver Digital Signal Processor (DSP). The data streams are routed into the DSP blocks for clock recovery, polarization combination, compensation of fast laser phase fluctuations, and recovery of the differential phase angles of the transmitted signal.

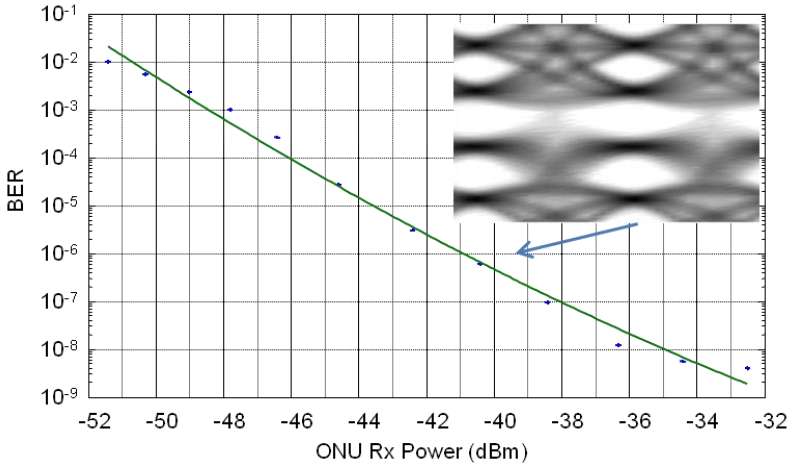

Figure 29: Bit Error curve for the ONU; Insert: Eye diagram at ONU

The resulting BER curve can be seen in Figure 29. A sensitivity of about -48 dBm for a BER of 10^{-3} was measured. Figure 29, insert, shows a typical 4 level differential phase eye diagram as received at the ONU. Both OLT and ONU are real-time capable. To demonstrate this, the data stream of a High Definition Video Server has been sent though the OLT downstream to the ONU where the data stream was recovered and transmitted to a standard video decoder. Real time video was observed and the onset of macroblocking was seen when the ONU input power was reduced below the video decoder's FEC level.

3.7 Wavelength Assignment

This section describes a simple method to manage wavelength assignment of a UDWDM system. In metro WDM systems, the operators haves access to both ends of the system and the configuration is by direct assignment, often via a separately management channel. In access systems, the situation is fundamentally different: until an ONU is physically connected to the fiber network and switched on, the operator has no prior configuration possibility. The ONU needs a method for identifying its assigned operating wavelength by itself and tune to it without prior communication with its associated OLT.

This ONU wavelength identification and assignment can be achieved by broadcasting a wavelength allocation table called "almanac" over all existing

wavelengths within the ODN. This table is unencrypted and superimposed over the encrypted traffic. At start-up, an ONU searches for any wavelength with a readable signal, waits for the almanac and extracts the unencrypted table, selects an unused wavelength, tunes there and locks on to the wavelength before opens communications with the OLT. The ONU does not transmit any light whilst reading the almanac, which allows the ONU to search an available wavelength without disturbing active ONUs in that PON.

In its simplest form, the almanac lists all possible wavelengths and tags them as "already in use", "available" and optionally "reserved". The table is hosted by the OLT and updated periodically. The amount of information transmitted depends on privacy requirements in the network. A more extensive almanac is possible, for example, to classify wavelength service attributes as well as vendor and service provider specifics, e.g., multi OLT environment in an open access system. The almanac is not intended for any management tasks beyond wavelength allocation. Such tasks are performed over the usual management channels (PLOAM or OMCI) once the ONU successfully establishes a stable communication link.

The almanac may also contain an identification of the current wavelength for each ONU for calibration purposes. The almanac is sent as a broadcast rather than over a dedicated management channel for two reasons: 1) to reduce the time required for an ONU to find the management information without prior knowledge; 2) to provide resilience against attempts to maliciously interfere with allocation information.

There is a risk that several new ONUs select the same wavelength at the same time, causing signal interference. This can be mitigated by randomizing the wavelength selection, by using exponential randomized backoff when transmitting first identification. As soon as the OLT can receive an ONU serial number, it should update the almanac to reserve this channel for the identified ONU for the duration of registration.

3.8 System capabilities enabled by wavelength flexibility

One important feature of UDWDM is its flexibility in spectrum assignment that allows OLT and ONUs to access different granularity of wavelengths, group of wavelengths, or wavelength bands. This feature enables several system capabilities which will be discussed here.

The first improved capability is system resilience. In case of fiber cut or OLT hardware issues, the users who lost service can be routed to a working OLT or PON card to continue receiving service at the same data rate if there are enough un-used wavelengths. If there are not enough un-used wavelengths, they can still receive service at a reduced data rate temporarily by using the wavelength sharing technique.

The second system capability addressed is power savings. During low traffic period of time, the number of active users is typically lower than that during peak hours. These users can be tuned to wavelengths associated with a few OTGs such that un-used OTGs can be switched off completely.

The third system capability is related to open access networks and infrastructures sharing. The major cost factor of metro-access networks deployment is in the fiber infrastructure. For new service providers entering the market, it is more cost effective to lease existing fiber from incumbent providers or utility companies who own the fiber infrastructure. In either case, several service providers would need to share the same fiber. With UDWDM, such sharing can be uniquely done in the physical layer by assigning different wavelength bands to each provider. Because of the fine wavelength spacing, each service provider has the ability to provide a large number of high data rate wavelengths within a narrow bandwidth - For example, 10 wavelengths each at 1Gbit/s within 50 GHz bandwidth.

4 Direct Detection and Coherent Optical OFDM

4.1 Optical OFDM

Optical OFDM (OOFDM) architectures include direct-detection OOFDM (DD-OFDM) and coherent-detection OOFDM (CO-OFDM). Next generation PONs will require Gbit/s aggregate downstream and upstream data-rate capacity, dynamic bandwidth allocation (DBA) for up to 1024 ONUs, and transmission distances of up to 100 km. Various PON architectures have been suggested including TDM-PON, WDM-PON, OFDM-PON, code division multiple access (CDMA) PON, and other hybrid options. WDM systems up to 40 Gbit/s capacity per channel have been utilized in backbone networks, and 100 Gbit/s interfaces are now commercially available. Fibre nonlinearities and CD become major sources of degradation >40 Gbit/s. On the other hand, OOFDM is a multi-carrier transmission technology that transmits high-speed data streams by using multiple parallel low-speed subcarriers that increases symbol duration and reduces inter-symbol interference (ISI). OOFDM is capable to transmit high-speed data streams using multiple spectrally-overlapping lower-speed subcarriers of high spectral efficiency (SE). Other advantages include robustness against CD and polarization mode dispersion (PMD). It can be used together with optical phase modulation formats such as DPSK, DQPSK, and QAM. OOFDM overcomes also inter-carrier interference (ICI) together with ISI by using cyclic prefix (CP) mitigating in this way both CD and PMD. OOFDM is also adaptable to channel conditions, and can provide robustness against Rayleigh backscattering (RB). It provides subcarrier granularities enabling flexible resource allocation, and could therefore provide flexible bandwidth in flex-grid networks. OOFDM enables smooth upgrading from low-speed to high-speed transmission by simply increasing subcarriers and spectrum without requiring major changes to system design. High spectrum efficiency can be achieved by OOFDM with overlapped subcarrier arrangement so the system capacity can be greatly increased. Link-adaptation capability of OOFDM provides even higher spectrum efficiencies as distance and channel condition-adaptive modulation (bit per symbol adjustment). Moreover, it provides symbol-by-symbol decision making for each sub-channel instead of requiring complex equalization algorithms to compensate for distortion. In addition, OOFDM allows energy-efficient operation to reduce

power consumption, and can be implemented by any system that uses adaptive modulation (i.e. AMOOFDM) [31]. Subcarriers can be dynamically switched on or off according to channel conditions and customer bandwidth requirements.

As shown in Figure 30 (a comparison of FDM with OOFDM), the OOFDM signal bandwidth consists of overlapping low bit-rate subcarriers. Orthogonality condition of overlap subcarriers is that the frequency spacing between any two subcarriers is the inverse of the baud rate. Orthogonality of subcarriers leads to high SE and increases the tolerance to CD. Close proximity of subcarriers creates a flat transmission channel. The use of low-bandwidth subcarriers OOFDM however results in high peak-to-average power ratio (PAPR). The PAPR increases susceptibility to nonlinear impairments, increases the energy consumption, and increases spectral overheads required for recovering information. A high PAPR is caused by symbol synthesis of multiple parallel subcarriers. Transceiver components must have a wide dynamic range so that high PAPR signal will not be distorted. In addition, OOFDM requires strict orthogonality between subcarriers; therefore, it is more sensitive to frequency and phase noise that could interfere with the orthogonality.

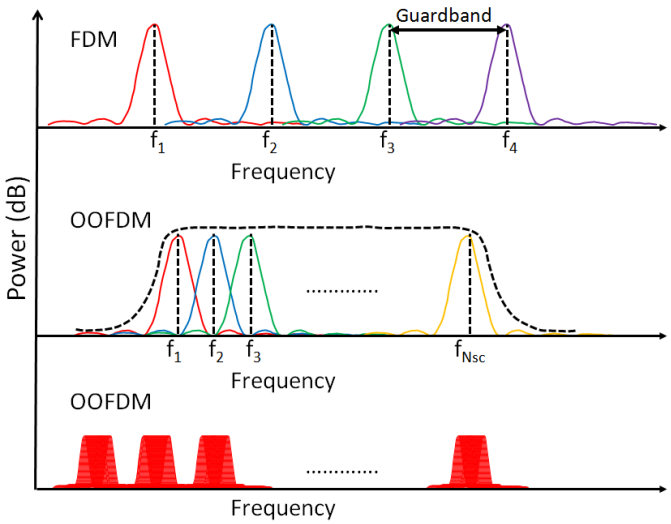

Figure 30 FDM and OOFDM spectrum analysis

4.1.1 Intensity-Modulation

Based on the aforementioned described OOFDM, in the DISCUS Metro/Core (MC) node, group of subcarriers are generated in the RF domain using OFDM with identical signal modulation format (such as QAM). Then the produced signal is modulated onto the *optical intensity* to come up with the downstream signal [32], [33], [34], [35] , [36]. The entire optical spectrum must be O/E converted at the receiver, while the different FDM windows are extracted in the electrical domain applying e.g. RF filtering and are subsequently electronically processed. Even if its performance is worst with respect to the *field modulation* approach which will be presented below (sometimes referred as "*optical* OFDM"), intensity-modulation OFDM is attractive due to its low-cost, which is usually suitable for short-haul applications [37], [38]. Figure 31 presents a block diagram of the OFDM transmitter for such case.

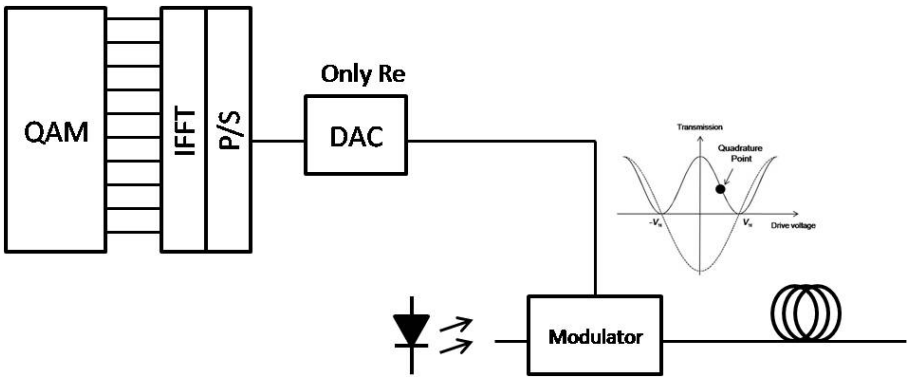

Figure 31 Intensity-modulation OFDM transmitter block diagram. The inset shows the bias point of the Mach-Zehnder modulator (MZM)

4.1.2 Field-Modulation

In this approach, *optical field modulation* is performed at the MC node side to produce the downstream signal. At the receiver side, optical filtering techniques can be applied to isolate the required FDM window - or even individual OFDM subcarriers from this window, in a more forward-looking scenario. Afterwards, only the filtered components need to be further processed in the electrical domain. It is clear that this approach imposes many challenges at the physical layer; however the benefits (some of which are bit-rate transparency, lower processing latency and improved energy-efficiency due to the reduced electronic processing effort) are important enough to justify investigating it in depth.

There are two forms of optical field-modulation OFDM. One is by up-converting the RF OFDM signal to a higher frequency by means of an RF-IQ-mixer. This RF-mixer will turn the complex-OFDM signal into a real one. Afterwards, the signal is sent to a simple Mach-Zehnder modulator (MZM), biased near to the null point in order to operate in the linear field region. However, it is important to mention that the optical spectrum has two sidebands that are symmetric over the optical carrier. A filter is used after the modulator to filter-out one band and reduce the power of the carrier [39], [40]. Figure 32 shows a block diagram of the RF up-conversion optical field-modulation OFDM.

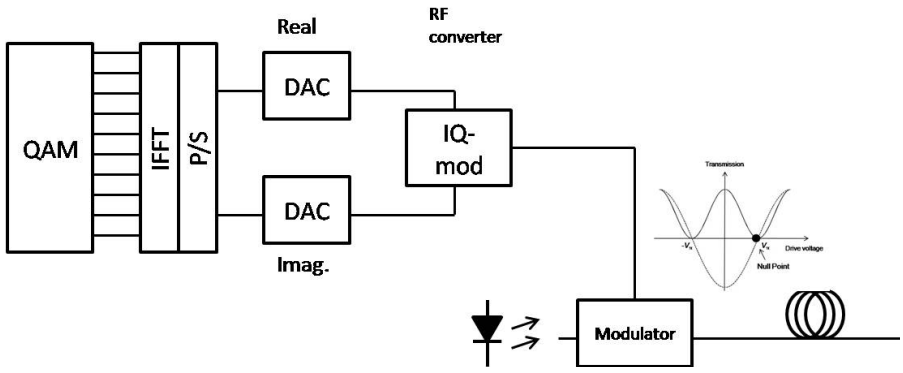

Figure 32 RF up-conversion optical field-modulation OFDM transmitter block diagram. The inset shows the bias point of the MZM

Another OFDM transmitter setup can be the use of a colorless transmitter incorporating a complex optical IQ modulator that comprises three MZMs for generating an optical signal from a complex RF electrical signal [38], [41]. By using this modulator there is no need of a filter to reject one of the OFDM bands since it already produces a single sideband (SSB) without optical carrier. Consequently, it increases the spectral efficiency, and receiver sensitivity [42], [43], [44]. Figure 33 presents the concept of optical field-modulation OFDM with a direct IQ optical modulator.

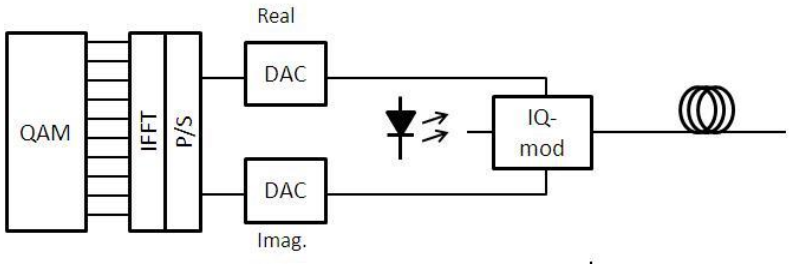

Figure 33 IQ optical mixer optical field-modulation OFDM transmitter

4.1.3 Direct-Detection Optical OFDM (DD-OOFDM)

The general well-known direct-detection receiver technique is depicted in Figure 34:

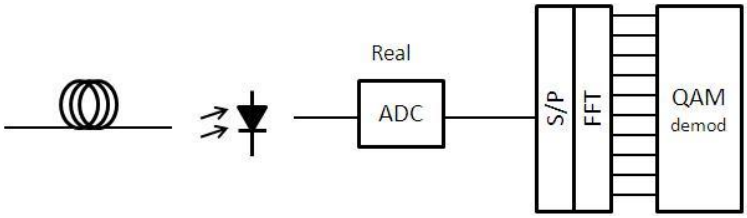

Figure 34 Direct-detection receiver block diagram

Several different DD-OOFDM configurations have been extensively demonstrated during the past few years.

4.1.4 Coherent Optical OFDM (CO-OFDM)

CO-OFDM has been widely regarded as a promising candidate for future long-haul high capacity transmission systems [45]. CO-OFDM was first proposed [46] and its study was extended in [38] for a 1000 km SSMF transmission reaching 8 Gbit/s. In [47], experimental work has reached 20 Gbit/s over 4160 km SSMF link using polarization division multiplexing (PDM). The two generic architectures of coherent detection OOFDM are illustrated in Figure 35:

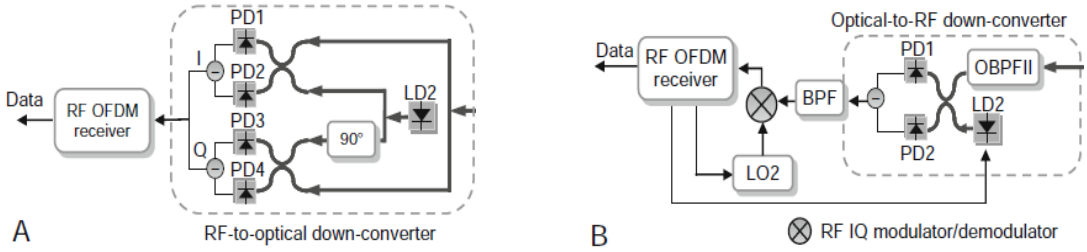

Figure 35 Generic architectures of CO-OFDM system: A. Homodyne architecture and B. Heterodyne architecture [48]

The spectral efficiency of CO-OFDM is high because it requires neither a transmitted optical carrier nor a gap between the optical carrier and the OFDM band. CO-OFDM also presents higher tolerance to PMD and CD because the system can be considered as a linear channel with constant phase shift which is automatically compensated in the symbol decision [49]. A typical CO-OFDM receiver is illustrated in Figure 36:

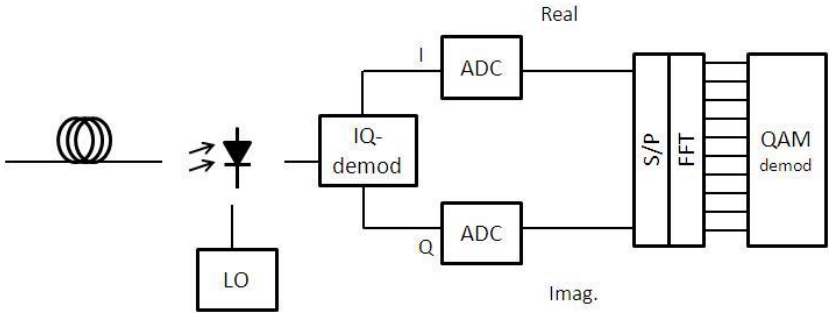

Figure 36 Coherent-detection OFDM receiver block diagram

The combined effect between coherent optical communications and OFDM are twofold. OFDM brings coherent systems computation efficiency and ease of channel and phase estimation. The coherent systems bring OFDM a much needed linearity in RF-to-optical (RTO) up-conversion and optical-to-RF (OTR) down-conversion.

For the homodyne architecture the detection process utilizes a six-port 90-degree optical hybrid and a pair of balanced photo-detectors. The main purposes of coherent detection are (i) to linearly recover the I and Q components of the incoming signal, and (ii) to suppress or cancel the common mode noise. The purpose of the four output ports of the 90-degree optical hybrid is to generate a 90-degree phase shift for I and Q components, and 180-degree phase shift for balanced detection. In the heterodyne architecture, the optical OFDM signal is first down-converted to an intermediate frequency LO2 and subsequently the electrical I/Q detection is performed [48].

The linear down-conversion process via coherent detection becomes quite obvious, and is based to the fact that the complex photocurrent is in essence a linear replica of the incoming complex signal that is frequency down-converted by a LO frequency. This linear down-conversion is of critical importance for OFDM modulation which assumes linearity in every stage of signal processing.

The first experimental demonstration of CO-OFDM systems is presented in [38], in which 128 OFDM subcarriers with a nominal data-rate of 8 Gbit/s are

successfully processed and recovered after 1000 km SSMF transmission. The experimental setup of the proposed CO-OFDM systems is illustrated in Figure 37.

The OFDM receiver signal processing involves (i) software down-conversion of the OFDM RF signal to baseband by using either a residual main carrier tone, or a pilot subcarrier tone, (ii) window synchronization using Schmidl format to identify the start of the OFDM symbol, (iii) phase estimation for each OFDM symbol, and (iv) constellation construction for each carrier and BER computation [38].

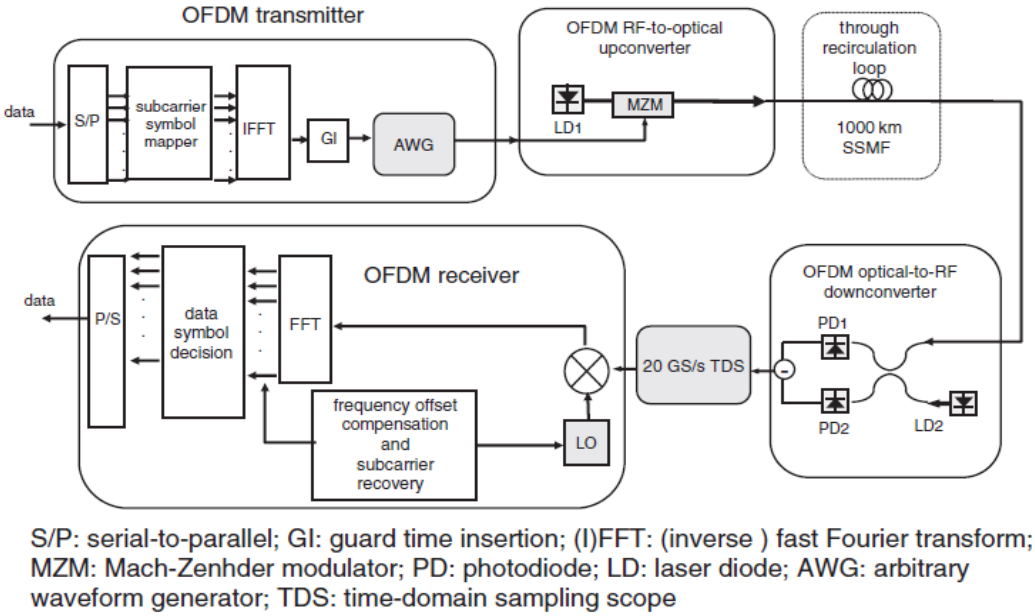

Figure 37 Experimental setup for CO-OFDM transmission [38]

More important, CO-OFDM is a modulation technique in which the hardware and software can be transformed seamlessly from the current generation to the next one whenever transmission speed is upgraded. Despite many applications for higher order modulation, due to the increased OSNR requirement and sensitivity to fibre nonlinearity, it was anticipated that QPSK 4-QAM or 2 bit per symbol modulation will be the dominant modulation for long-haul transmission systems as a satisfactory compromise between spectral efficiency and system performance [38].

4.1.5 Comparison between CO-OFDM and DD-OOFDM

The optical bandwidth requirements for DD-OOFDM are determined both by the OFDM band and the gap between the OFDM band and the optical carrier. The width of this gap is typically equal or larger than the width of the OFDM band. The OFDM band itself has a bandwidth of almost half the gross data rate [50].

On the other hand, in CO-OFDM systems the transmission of an optical carrier is not required; nevertheless for adaptation purposes the transmission of a

residual carrier with lower power may be advantageous. Therefore, optical bandwidth requirements for CO-OFDM are much lower compared to DD-OOFDM because of transmitting no optical carrier with the required gap to the OFDM band in addition to the modulated subcarriers. Moreover, CO-OFDM requires less OSNR than DD-OOFDM [51] and by using sophisticated post-detection DSP; its CD tolerance is increased making it more valuable for longer distances in contrast with DD-OOFDM [52]. By employing higher-level of subcarrier modulation the spectral efficiency can be increased. For the case of polarization multiplexed systems, the spectral efficiency can be doubled even when low signal modulation formats are applied, such as QPSK. The aforementioned statement reveals that the spectral efficiency of CO-OFDM is improved compared to DD-OOFDM; however, its hardware implementation is more complex and not cost-effective. Finally, it is polarization dependent and requires a narrow linewidth oscillator which is sensitive to phase noise and frequency offset [52]. This restricts its use in cost-sensitive networks [52].

4.2 Optical OFDM for Long-Reach PON

For all the results presented in this section, the OFDM transceivers are similarly designed to those described in [38]. A DWDM-OFDM configuration has been considered: in the transmitters, binary data sequences are encoded serially by using 64-QAM in order to achieve a bit-rate of 100 Gbit/s in a single downstream wavelength. A serial-to-parallel (S/P) converter truncates the encoded data to subcarriers. An inverse fast Fourier transform (IFFT) is then applied to the subcarriers. When intensity-modulation with direct-detection (IM/DD) is considered then Hermitian symmetry property is applied in order to generate real-valued OFDM symbols as depicted in Figure 38 for the OLT and ONU. These symbols are serialized to form a signal sequence, to which signal clipping is applied for the purpose of limiting the OFDM signal power. At the final stage DACs are used to convert the digital data sequences into analogue signal waveforms, which drive the lasers and generate the OOFDM signal waveforms. In the receiver, the optical signals are converted into electrical signals using PIN-FET photodiodes and passing through the corresponding electrical low-pass filters (LPFs). Afterwards, the converted electrical signals encounter the inverse of that described in the transmitters. It should be noted that for the IM/DD case, the encoder creates the OFDM symbols with the original data in the positive frequency bins while the complex conjugate of the data in the negative frequency bins. In addition, in all cases no power is contained in the first subcarrier close to the signal OFDM baseband to avoid significant interference with the optical component.

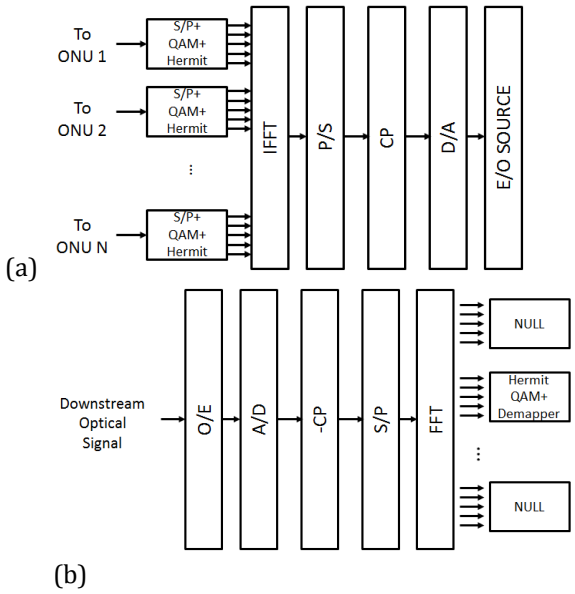

Figure 38 Example of (a) OLT and (b) ONU downstream (DS) OFDM LR-PON equipment

The targeted bite-error-rate (BER) per channel is always 10^{-3}. The number generated OFDM subcarriers is 128. The CP is taken large at 25% to virtually eliminate inter-symbol interference (ISI). The DAC/ADC clipping ratio and quantization bits are taken at optimum values of 13 dB and 8, respectively [38]. EDFAs are adopted having 20 dB gain and 5 dB noise figure. The extinction ratio (ER) of the Mach-Zehnder modulator (MZM) is 25 dB. The transmitted wavelength is set at 1552.5 nm.

4.2.1 100 Gbit/s downstream CO-OFDM

In Figure 39 the DISCUS configuration for dense urban scenario using a single CO-OFDM channel at 100 Gbit/s is depicted.

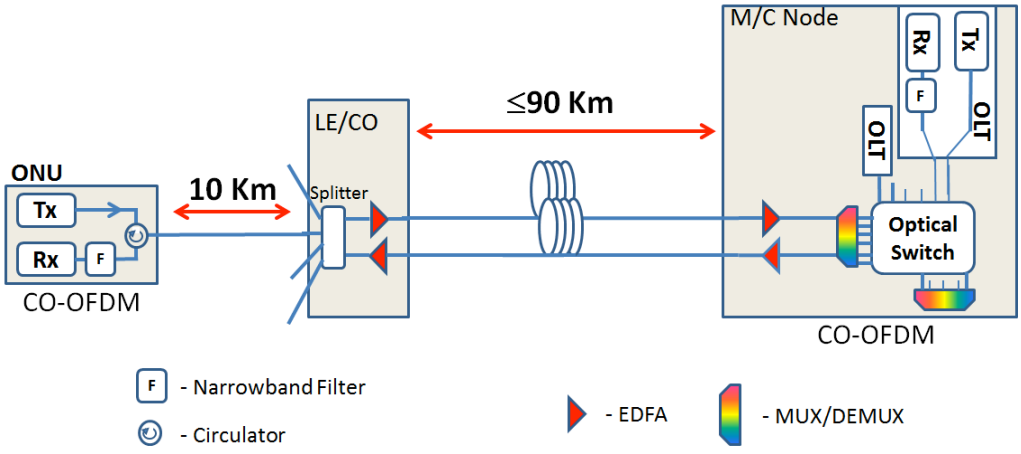

Figure 39 DISCUS configuration for dense urban scenario using a single CO-OFDM channel at 100 Gbit/s

In Figure 40, the power margin versus total transmission distance (back-haul + distribution section) for downstream CO-OFDM LR-PON using 64-QAM at a bit-rate

of 100 Gbit/s is illustrated for different split ratios, i.e. 1:64, 1:128, and 1:256. It is revealed from Figure 41 that up to about 9 dB of power margin is available at a total transmission distance of 100 km (90 km + 10 km) for the downstream LR-PON configuration at a minimum 1:64 split ratio.

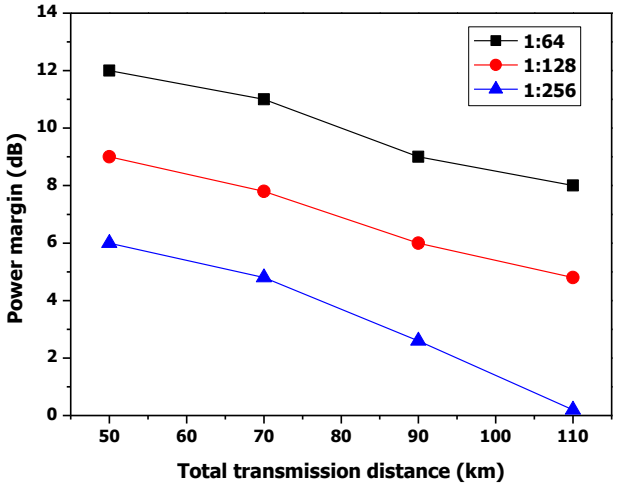

Figure 40 Power margin vs. total transmission distance (back-haul + distribution section) for downstream CO-OFDM LR-PON using 64-QAM at a bit-rate of 100 Gbit/s

4.2.2 Direct-Detected LR-OFDM PON using Cost-Effective High-speed GaAs IQ Electro-Optic Modulators

LR-PONs have been recently proposed as an economically viable solution [53] for future-proof next-generation access networks. In LR PONs the OLT is placed at a distance of up to 100 km and the transmitted signal is sufficiently amplified in an intermediate point to compensate both the transmission and distribution losses, allowing feeding up > 512 ONUs [54]. OOFDM has been introduced to LR PONs for improving spectral efficiency [55], [56]. Practical OOFDM transmission will require an electro-optic (EO) modulator technology capable to blend high-speed operation, scalability and cost-effectiveness. So far, research demonstrations of OOFDM transmission have relied heavily on two different technologies, i.e. $LiNbO_3$ and InP [57], [58]. However, these two technologies exhibit different disadvantages that are critical in practical high capacity OOFDM systems, where device scalability is of prime concern. $LiNbO_3$ devices exhibit a large chip size which complicates array integration, whereas InP chips are costly due to the small InP wafers.

Below the applicability of this technology for LR-PON is presented. The applicability study is performed over a low-cost LR direct-detected multiband (MB) OFDM-PON system. The applicability study demonstrates OOFDM downstream transmission of 40 Gbit/s LR-PON over 100 km supporting up to 1024 users in this section. The high yield fabrication process combined with the availability of large 6-inch wafers and potential fabrication in large foundries renders GaAs a promising future-proof technology for scalable cost-efficient next-generation LR-OFDM-PONs.

- *GaAs IQ Modulator Testing*

GaAs modulators have been fabricated using u²t Photonics foundry-based fabrication process incorporating 6-inch semi-insulating GaAs in the processing of the modulators. The modulator chip integrates an array of six parallel IQ modulators as a single tile, which is shown in the Figure 41 [59].

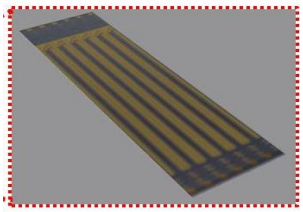

Figure 41 Example of a GaAs modulator chip under test which integrates six parallel GaAs IQ modulators as a single tile [59].

- *Cost-effective GaAs Modulator Applicability in LR-OFDM-PONs*

The application in LR-PON of the fabricated MZM was analyzed through simulation using VPI Transmission Maker®. This commercial simulator allows loading the measured parameters of the MZM, such as its frequency response and its ER, ensuring a realistic model of the device under test (DUT). The simulated architecture is presented in Figure 43, which corresponds to a typical direct-detection MB-OFDM transmission system referenced with a combined de-multiplexer (DEMUX)/splitter distribution, whose parameters are presented in Table 4.1. The MB-OFDM signal had four tributaries, each one carrying a bit-rate of 10-Gbit/s, and consisting of 64 subcarriers that were modulated with QPSK. A 12.5% CP was added to each subband to compensate fibre CD. The interband frequency spacing was set to 7.5 GHz and the intermediate frequency of the first subband was fixed to 7.5 GHz, resulting in the spectrum shown in Figure 42. The conversion to the optical domain was performed using a pair of MZMs whose parameters were set according to the characterization in [59]. The MZMs were configured in IQ-scheme, producing a SSB modulation and avoiding optical filtering. The modulated optical signal was amplified and transmitted over a 90 km standard single-mode fiber (SSMF) span, representing the back-haul section of the LR-PON. The parameters of the SSMF are set to: fiber loss (α) = 0.2 dB/km, dispersion (D) = 16 ps/nm/km, dispersion slope (S) = 0.06 ps/km/nm^2, nonlinear coefficient (γ) = 1.2 1/W/km, polarization mode dispersion (PMD) = 0.1 ps/km$^{0.5}$. The signal was amplified again. The adopted link included EDFAs with noise figure of 5 dB configured in power clamped mode which allowed to directly controlling the output power. Following amplification, the signal was filtered to model the channel selection of the DEMUX. The SSB was then attenuated, emulating the losses of the distribution splitters, and transmitted over a second SSMF span of 10 km. Afterwards, the signal was directly-detected in a PD at the ONU and down-converted to baseband where it was processed. Simulations were carried out using different amplifiers in order to use the lowest possible gain, reducing the power consumption which is a crucial issue throughout the DISCUS project. In addition, the results using the fabricated MZM were compared to an ideal benchmark MZM model exhibiting a

flat response and an ER of 40 dB.

Table 12 LR-OFDM-PON Transceiver Parameters

Parameter	Value
Total signal bit rate	40-Gbit/s
Number of subbands	4
CP length	12.5%
Subcarrier number	64
Interband spacing	7.5 GHz
DAC/ADC Quantization bits	8
DAC/ADC Clipping ratio	13 dB
MUX/DEMUX Insertion loss	3 dB
EDFA Gain	20 dB
EDFAs noise figure	5 dB

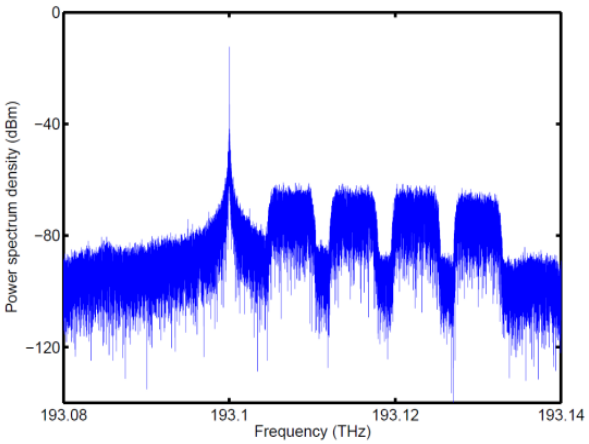

Figure 42 Received optical spectrum of four OFDM subbands.

The first step was the optimization of the driving voltage, which is shown in Figure 44 (left). As expected, for low driving voltage elevate BER are obtained due to the low SNR, while for high driving voltages, nonlinear distortion becomes dominant. The optimum trade-off between noise and nonlinearities was obtained closed to 0.35 V for 20 mW amplifier output power and 0.32 V for 100 mW output powers. This makes sense since at higher amplifier gain the effects of the noise are reduced and the curves are shifted toward the left. In addition, the optimum driving voltage is the same for both the GaAs and the benchmark MZMs. Once the driving voltage was optimized, we simulated the BER for different distribution network losses in the similar way as performed in [60].

For low distribution losses as revealed in Figure 44, the nonlinear effects of the fibre are significant and, hence, the BER is improved as the losses increased. After a given loss value (which is highly dependent on the output power of the amplifiers), the BER started to rise, meaning that the system was limited by noise. The effect of the output power of the amplifier is evident from Fig. 4.15 (right). Results also reveal that differences between the fabricated and the benchmark are only appreciable at low distribution networks, but there is no power penalty at BER close to 10^{-3}. Comparing the proposed system with a complete splitter-based-distribution system in [60], the MB approach allows substituting one of the splitter by a DEMUX, reducing the losses for the same split size by 6 dB. Therefore, the distribution losses for 1024 split size are 34.5 dB, and for 512 split size 31.5 dB. Assuming a forward-error correction (FEC) limit at

10^{-3}, this implies that a split size of 1024 can be achieved using 100 mW output power. However, for 50 mW optical amplifier output power, the maximum number of users that can be served is reduced to 512, as can be appreciated in Figure 44(right).

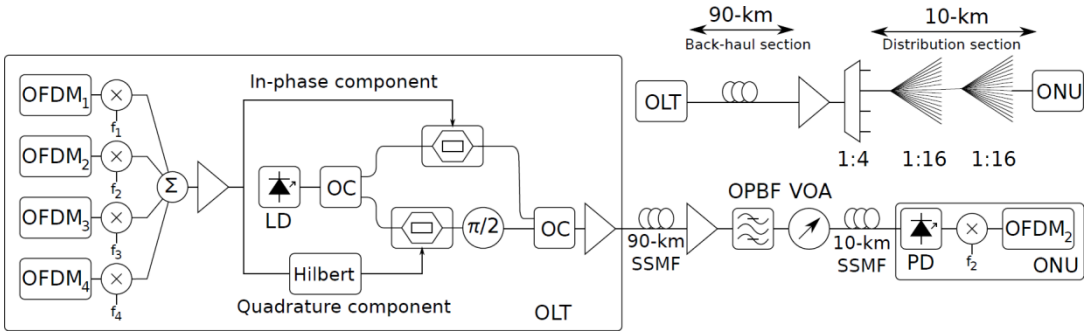

Figure 43 LR-OFDM-PON reference architecture for up to 1024 users. Inset: OFDM: orthogonal frequency-division multiplexing, OPBF: optical pass-band filter, VOA: variable optical attenuator, PD: photodiode, ONU: optical network unit, OLT: optical line terminal, OC: optical coupler, LD: laser diode, SSMF: standard single-mode fiber

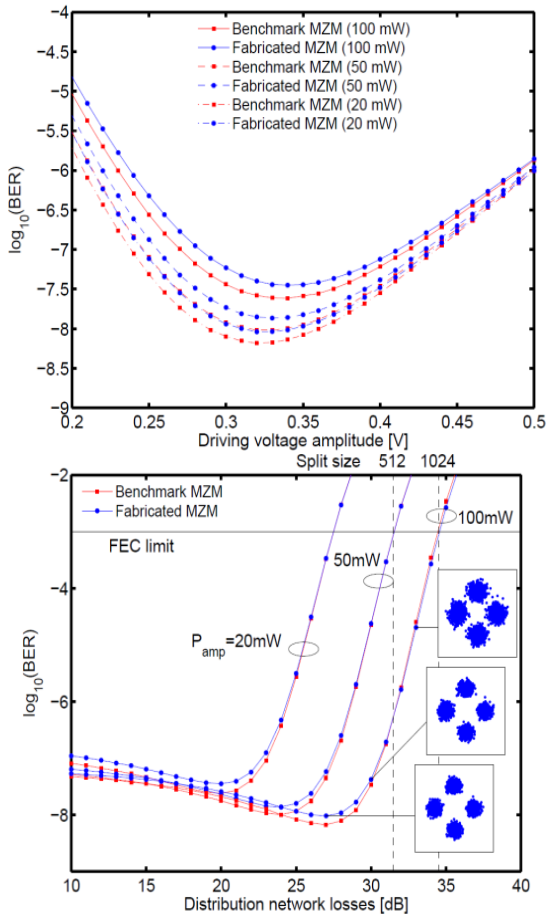

Figure 44 (Left) BER vs. driving voltage amplitude for benchmark (red) and fabricated (blue) MZMs under different applied driving voltage. (Right) BER vs. distribution network losses for benchmark (red) and fabricated (blue) MZMs for different P_{amp} at 512 and 1024 split-way. Inset: Received QPSK constellation diagrams for different distribution network losses

4.3 Techno-Economic OFDM Model and Comparisons with Legacy PONs

Techno-economic cost model and software has been created for comparing the various optical access solutions. Given certain network design parameters, the software automatically dimensions the network, calculates quantity of equipment required, and costs the network. Using this model we can study the network costs for various architectures for different central office (CO) area geo-types and take-up rates. Therefore we can study the feasibility of providing universal capability to all sectors of the community in widely varying geographical locations. The base cost data for component and sub-systems were obtained from public domain sources. The fibre, duct, and cable costs were obtained from Analysys Mason [61]. Other costs were obtained from manufacturers' websites. Figure 45 shows a flow diagram of the cost model. Depending on the network being modelled, the program dimensions the network, calculates splitter sizes, and quantity of equipment needed. The program then calculates costs in terms of infrastructure costs, electronic equipment costs, ONU costs, drop costs, and the access network equipment costs. Appropriate learning curves are applied for each technology. Cash flow curves are obtained by subtracting expenses (capital expenditure, operational expenditure etc.) from the income from revenue in that year and discounting back to the start year, assuming a discount rate of 11%.

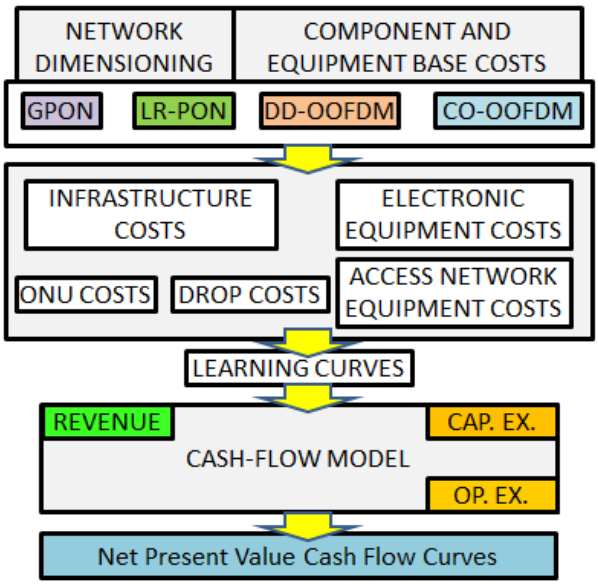

Figure 45 Flow diagram of techno-economic cost model

A learning curve of 80% was assumed for the optical and electronic equipment; optical external plant and street furniture were assumed to decline with a learning curve of ~95%. Revenue growth was assumed to be ~4% per year, the historical rate for the network operator industry in Europe. Starting with a specified CO population, splitter sizes for different stages in the network

were calculated. This allows us to calculate the number of LR-PONs required in a CO area. The number of PONs per CO is then calculated by dividing the total CO population by the number of customers per PON (e.g. 1024 in the case of LR-PON), using a fill factor of 80% to allow some flexibility. For the metro node (assuming two metro nodes per PON for protection purposes), a total maximum bandwidth can be calculated from maximum downstream and upstream bandwidth for each customer. The number of OLT cards can be calculated from the number of PONs and the number of OLTs per card. Each OLT terminates a LR-PON. The number of 10GE ports is calculated from the maximum total bandwidth and the WDM payload per 10GE wavelength. The number of switch cards required is calculated from the total maximum bandwidth divided by the capacity per switch card (10 Gbit/s). The number of shelves is calculated from the number of cards per shelf. The number of GE port cards can be calculated from the number of GE ports divided by number of ports per GE port card. The number of 10G XFP modules is the number of 10GE port cards multiplied by number of XFP modules per port card. It is assumed that all ports are short-reach providing across the floor connection to metro-node switch. For each shelf, there is a management and software card, and for each rack a power supply. The metro-node equipment and buildings are not included in the model except for the backhaul transmission system terminating equipment (i.e. GE and 10GE line cards). Cost of the distribution points can be calculated from the cost of the housing for the splitters and installation costs. The number of linecards can be calculated from bandwidth requirements, and the number of fiber cables required. LR-PON amplifier modules include 2 or 4 EDFAs depending on protection, housing and power, etc. requirements. The number of amplifier modules can be calculated from the total number of LR-PONs.

Assuming a certain distribution point (DP) splitter size we can calculate the number of DPs. This can be calculated from the CO population, and the average number of customers passed per DP. The number of DP housings is assumed to be equal to the number of DPs. From the number of cabinets and the number of PONs, the splitter sizes for a CO can be calculated. The cabinet splitter sizes can be calculated from the LR-PON splitter size (1024), the DP splitter size (32), and the CO splitter size. Backhaul cable costs can be calculated from the number of fibres required. This is calculated from the number of PONs. From the number of fibres, the number of 12-fibre units can be calculated, and from that the cable sizes provided is calculated. Available cable sizes are 12, 24, 48, 96, 144, and 240 cable sizes. Cable costs are found from [61]. The cost per km can be calculated that includes the cable costs, duct, and subduct costs as well as installation costs. Assuming a certain amount of duct build, the backhaul cable costs can be calculated. The LR-PON metro-node has fewer PONs therefore the total number of fibres and hence the backhaul costs is less. The e-side is the segment from the cabinet to the CO. The d-side is the segment from the cabinet to the DP. The mean d-side and e-side distances are obtained from [61]. The e-side consists of the A and B segments, where the A-segment is 25% of the e-side distance, and B-segment is 75%. In the A-segment, we assume that there are 4 cable routes from the CO towards the cabinets. This means that at a certain distance from the CO, at a fibre flexibility points, the cable route splits into individual routes with their associated ducts, connected to each cabinet. Because the number of B-segment

ducts is large, equal to the number of cabinets, this cost can be significant. The duct distances to each cabinet varies from duct-to-duct. However mean distances can be obtained from [61]. The A-segment cost from the CO can be calculated from the total number of splits out of the CO towards the cabinets. This is calculated by multiplying the number of PONs by the CO splitter size for that PON. We assume that there is there is 1 fibre per PON, including some flexibility factor to make sure there are enough fibres. From the total splits, for each of the 4 routes out of the CO, we can find the number of 12 fibre units required. The cable size for the A-segment can be calculated from calculating the number of 12-units required per route, and choosing from {12, 24, 48, 96, 144, and 240}. If the cable size required is greater than 240, we just multiply by 12.

The number of cables per route can be calculated by dividing the number of fibres per route by the cable size that can be provided. The total number of cables for all 4 routes can be calculated by multiplying this by 4. The A-segment cost is therefore the A-segment distance, multiplied by the cost/km for the cable, and ducts, taking into consideration the duct build, multiplied by 4. The B-segment cost can be calculated from the B-segment distance multiplied by the number of cabinets, and the cost mainly due to the number of ducts required.

Similarly the d-side consists of C and D segments, where the C-segment is 85%, and D-segment is 15% of d-side distance. Therefore at the fibre flexibility point on the d-side the cable route splits into individual ducts for each DP.

The C-segment cost can be calculated by assuming that there are 4 cable routes from the cabinets to the DPs. Therefore the total C-segment costs is the total number of cable routes (4x number of cabinets) multiplied by the cost per km for the cable size required and the C-segment distance. From the number of 12-unit fibres required, we can calculate the cable size {12, 24, 48, 96, 144, and 240} that can be provided, and from the associated cost per km, the C-segment cost. The D-segment cost can be calculated from the number of ducts calculated from the number of DP's and the D-segment distance, and the cost per km. The drop side could similarly be divided into E and F sections. However in this simplified model we assumed that the cost is length independent, and instead depends on how many sites an engineer is able to connect in one day.

The customer premises equipment (CPE) including the ONU are connected to the DP on a just-in-time basis. The total number of customers connected is equal to the take-up rate multiplied by the number of customers in the CO area. In this case, if the take-up rate is 30%. The total cost for each network is calculated by adding the total costs for each stage in the network as well as the cabling and infrastructure costs. We assume that the 'cost per customers passed' is the total cost divided by the number of customers and is paid up-front, i.e. the network is built until it reaches the DPs. The 'cost per customers connected' includes the just-in-time cost of adding the drops to the customers.

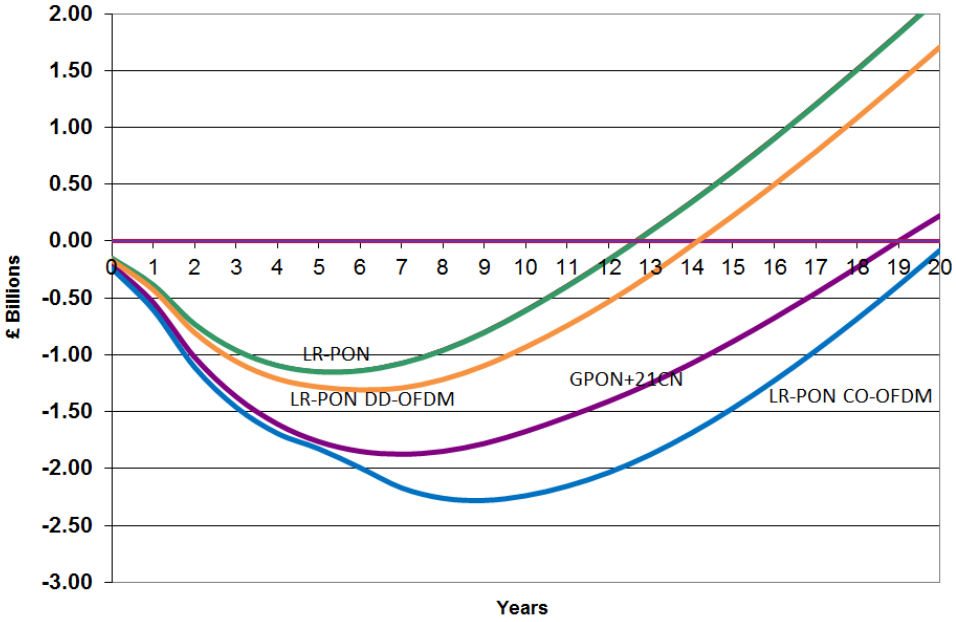

Figure 46 Techno-economic comparisons

Cash flow curves are calculated by subtracting expenses (capital expenditure, operational expenditure etc.) from income from revenue in that year and discounting back to the start year, assuming a discount rate of 11%. A learning curve of 80% was assumed for the optical and electronic equipment. Optical external plant and street furniture were assumed to decline with a learning curve of ~95%. Operational costs include manpower and replacement of network equipment after wear-out. We define learning curve as the percentage reduction in the price of a product when the production volume doubles. For example, typically electronic systems have learning curves of ~80%, meaning that the price of a product at volume V reduces to 80% of its price when the volume doubles to 2V. As industry learns how to manufacture a product the price decreases. Newer technologies generally sit on faster curves. Older technologies sit on slower learning curves, because not much learning occurs as production volume increases. Revenue growth is assumed to be ~4% per year, the historical rate for the network operator industry in Europe. The model allows for the growth rate to be toggled on and off so that comparisons without revenue growth can also be made.

Figure 46 shows an initial cash flow comparison between the direct detection and coherent detection and OFDM technologies using the LR-PON architecture.

5 References

[1] from ITU-T G.989.2 draft Recommendation.

[2] W. Poehlmann et al., *Demonstration of Wavelength-Set Division Multiplexing for a Cost Effective PON with up to 80 Gbit/s Upstream Bandwidth*, ECOC 2011, paper We.9.C.1.

[3] Doutje van Veen et al., *System Demonstration of a Time and Wavelength-Set Division Multiplexing PON*, ECOC2013, paper We.3.F.2.

[4] B. Baekelandt, C. Melange, J. Bauwelinck, P. Ossieur, T. De Ridder, Xing-Zhi Qiu, J. Vandewege, "OSNR Penalty Imposed by Linear In-Band Crosstalk Caused by Interburst Residual Power in Multipoint-To-Point Networks," Photonics Technology Letters, IEEE , vol.20, no.8, pp.587,589, April15, 2008.

[5] C. Antony, G. Talli, P. D. Townsend, J. Bauwelinck, D. W. Smith, I. Lealman, "High extinction switching of SOAs for in-band crosstalk reduction in PON," Electronics Letters , vol.44, no.14, pp.872,873, July 3 2008.

[6] Ossieur, P.; Antony, C.; Naughton, A.; Clarke, A.M.; Krimmel, H. -G; Xin Yin; Xing-Zhi Qiu; Ford, C.; Borghesani, A.; Moodie, D.; Poustie, A.; Wyatt, R.; Harmon, B.; Lealman, I.; Maxwell, G.; Rogers, D.; Smith, D.W.; Smolorz, S.; Rohde, H.; Nesset, D.; Davey, R.P.; Townsend, P.D., "Demonstration of a 32 512 Split, 100 km Reach, 2 32 10 Gb/s Hybrid DWDM-TDMA PON Using Tunable External Cavity Lasers in the ONUs," Lightwave Technology, Journal of , vol.29, no.24, pp.3705,3718, Dec.15, 2011.

[7] J. Buus and E. J. Murphy, “Tunable lasers in optical networks,” J. Lightw. Technol., vol. 24, no. 1, pp. 5–10, Jan. 2006.

[8] B. Mroziewicz, “External cavity wavelength tunable semiconductor lasers—A review,” Opto-Electron. Rev., vol. 16, no. 4, pp. 3Buus06–366, 2008.

[9] T. Mukaihara, Y. Nakagawa, H. Nasu, H. Kambayashi, M. Oike, S. Yoshimi, T. Kurobe, T. Kimoto, K. Muranushi, T. Nomura, and A. Kasukawa, “High power, low noise, low power consumption, 25 GHz□180 ch. thermally tunable DFB laser module integrated with stable wavelength monitor,” presented at the Eur. Conf. Optical Communication (ECOC), Rimini, Italy, 2003, Paper We4.P.81.

[10] B. Pezeshki, E. Vail, J. Kubicky, G. Yoffe, S. Zou, J. Heanue, P. Epp, S. Rishton, D. Ton, B. Faraji, M. Emanuel, X. Hong, M. Sherback, V. Agrawal, C. Chipman, and T. Razazan, “20-mW widely tunable laser module using DFB array and MEMS selection,” IEEE Photon. Technol. Lett., vol. 14, pp. 1457–1459, Oct. 2002.

[11] V. Jayaraman, A. Mathur, L. A. Coldren, and P. D. Dapkus, “Extended tuning range in sampled grating DBR lasers,” IEEE Photon. Technol. Lett., vol. 5, pp. 489–491, May 1993.

[12] H. Ishii, Y. Tohmori, Y. Yoshikuni, T. Tamamura, and Y. Kondo, "Multiple-phase shift super structure grating DBR lasers for broad wave- length tuning," IEEE Photon. Technol. Lett., vol. 5, pp. 613–615, Jun. 1993.

[13] A. J. Ward, D. J. Robbins, G. Busico, E. Barton, L. Ponnampalam, J. P. Duck, N. D. Whitbread, P. J. Williams, D. C. J. Reid, A. C. Carter, M. J. Wale, "Widely Tunable DS-DBR Laser With Monolithically Integrated SOA: Design and Performance", IEEE Journal Of Selected Topics In Quantum Electronics, Vol. 11, No. 1, January/February 2005.

[14] J. O. Westerstrom, G. Sarlet, S. Hammerfeldt, L. Lundqvist, P. Szabo, and P. J. Rigole, "State-of-the-art performance of widely tunable mod- ulated grating Y-branch lasers," presented at the Optical Fiber Conf. (OFC), Los Angeles, CA, Feb. 2004, Paper TuE2, pp. 389–391.

[15] R. Phelan, W.-H. Guo, Q.-Y. Lu, D. Byrne, B. Roycroft, P. Lambkin, B. Corbett, F. Smyth, L. P. Barry, B. Kelly, J. O'Gorman, J. F. Donegan, "A Novel Two-Section Tunable Discrete Mode Fabry-Perot Laser Exhibiting Nanosecond Wavelength Switching", Vol 44, JQE, pp331-337, 2008.

[16] R. Murano, W. Sharfin, and M. Cahill, "Tunable 2.5Gb/s Receiver for Wavelength-Agile DWDM-PON," in Optical Fiber Communication Conference/National Fiber Optic Engineers Conference, OSA Technical Digest (CD) (Optical Society of America, 2008), paper PDP32.

[17] S. Porto, C. Antony, G. Talli, P. Ossieur and P.D. Townsend, "Requirements for adaptive electronic dispersion compensation in burst-mode systems", Optical Fiber Conference (OFC'2013), Paper OTh3B.5, March 2013.

[18] P. Ossieur, N.A. Quadir, S. Porto, C. Antony, W. Han, M. Rensing, P. O'Brien and P.D. Townsend, "A 10Gb/s linear burst-mode receiver in 0.25 m SiGe BiCMOS", IEEE J. Solid-State Circuits, vol. 48, Feb. 2013.

[19] "Implementation agreement for integrated dual polarization intradyne coherent receivers," OIF, IA OIF-DPC-Rx-01.0, April 2010.

[20] P. Ossieur, N. A. Quadir, S. Porto, M. Rensing, C. Antony, P. O'Brien, Y (Frank) Chang, and P. D. Townsend, "A 10G Linear Burst-Mode Receiver Supporting Electronic Dispersion Compensation for Extended-Reach Optical Links, " Optics Express, vol. 19, iss. 26, pp. 604–610, Dec 2011.

[21] Govind P. Agrawal, *Fiber-Optic Communications Systems*, 3rd Edition, 2002.

[22] D. van Veen, V. Houtsma, P. Winzer, and P. Vetter, "26-Gbps PON Transmission over 40-km using Duobinary Detection with a Low Cost 7-GHz APD-Based Receiver," in ECOC 2012, paper Tu.3.B.1.

[23] D. Chang, F. Yu, Z. Xiao, Y. Li, N. Stojanovic, C. Xie, X. Shi, X. Xu, and Q. Xiong, "FPGA Verification of a Single QC-LDPC Code for 100 Gb/s Optical Systems without Error Floor down to BER of 10-15," OFC 2011, paper OTuN2.

[24] D. Lavery, M. Paskov and S. J. Savory, "Spectral Shaping for Mitigating Backreflections in a Bidirectional 10 Gbit/s Coherent WDM-PON," in OFC, 2013.

[25] Savory and S. J. Savory, “Digital Coherent Optical Receivers :Algorithms and Subsystems,” IEE Journal of selected topics in quantum electronics, vol. 16, no. 5, pp. 1164-1179, 2010.

[26] M. G. Taylor, “Phase Estimation Methods for Optical Coherent Detection Using Digital Signal Processing,” Journal of Lightwave Technology, vol. 27, no. 7, pp. 901-914, 2009.

[27] H. Wang, Y. Lu and X. Wang, “Channelized Receiver with WOLA Filterbank,” in International Conference on Radar, 2006. CIE '06, 2006.

[28] F. J. Harris, C. Dick and M. Rice, “Digital Receivers and Transmitters Using Polyphase Filter Banks for Wireless Communications,” IEEE Transactions on Microwave Theory and Techniques, vol. 51, no. 4, pp. 1395-1412, 2003.

[29] S. Smolorz, E. Gottwald, H. Rohde, D. Smith and A. Poustie, “Demonstration of a Coherent UDWDM-PON with Real-Time Processing,” in OFC, 2011.

[30] L. Kazovsky, G. Kalogerakis and W. T. Shaw, “Homodyne Phase-Shift-Keying Systems: Past Challenges and Future Opportunities,” Journal of Lightwave Technology, vol. 24, no. 12, 2006.

[31] E. Giacoumidis, J. L. Wei, X. L. Yang, A. Tsokanos, J. M. Tang, "Adaptive-Modulation-Enabled WDM Impairment Reduction in Multichannel Optical OFDM Transmission Systems for Next-Generation PONs," IEEE Photonics Journal, vol. 2, pp. 130 - 140, 2012

[32] M. Schuster, S. Randel, C.A. Bunge, et al. "Spectrally efficient compatible single-sideband modulation for OFDM transmission with direct detection", IEEE Photon. Technol. Lett., vol. 20, pp. 670-672, 2008

[33] N.E. Jolley, H. Kee, P. Pickard, J. Tang, K. Cordina, "Generation and propagation of 1550nm 10 Gbit/s optical orthogonal frequency division multiplexed signal over 1000m of multimode fibre using a directly modulated DFB," Proc. OFC 2005, paper OFP3.

[34] J. Armstrong, "OFDM for optical communications," IEEE J. Lightwave Technol., vol. 27, no. 3, pp. 189-204, 2009

[35] E. Giacoumidis, J.L. Wei, X.Q. Jin, J.M. Tang, "Improved transmission performance of adaptively modulated optical OFDM signals over directly modulated DFB laser-based IMDD links using adaptive cyclic prefix," Optics Express, vol. 16, pp. 9480-9494, 2008

[36] J.M. Tang, K.A. Shore, "30 Gb/s signal transmission over 40-km directly modulated DFB-laser-based single-mode-fibre links without optical amplification and dispersion compensation," IEEE J. Lightwave Technol., vol. 24, pp. 2318-2327, 2006

[37] A. Ali, J. Leibrich, W. Rosenkranz, "Spectrally efficient OFDM-transmission over single-mode fibre using direct detection," 13th International OFDM workshop (InOWo'08), 27-28 Aug 2008, Hamburg, Germany

[38] B.J.C. Schmidt, A.J. Lowery, J. Armstrong, "Experimental demonstrations of 20 Gbit/s direct-detection optical OFDM and 12 Gbit/s with a colorless transmitter," Proc. OFC 2007, paper PDP18

[39] T. Omiya, H. Goto, K. Kasai, M. Yoshida, and M. Nakazawa, "24 Gbit/s, 64 QAM-OFDM coherent transmission with bandwidth of 2.5 GHz," in Proc. ECOC 2008,Vienna, Austria, paper 1.3.2

[40] H. Takahashi, "Coherent OFDM transmission with high spectral efficiency," in Proc. ECOC 2009, Vienna, Austria, paper 1.3.3

[41] C.T. Lin, Y.M. Lin, J. Chen, S.P. Dai, P.C. Peng, P.T. Shih, and S. Chi, "Generation of direct-detection optical OFDM signal for radio-over-fibre link using frequency doubling scheme with carrier suppression," in Proc. OFC 2008, paper OMM5

[42] Abdulamir Ali, et al. "Spectrally Efficient OFDM-Transmission over Single-Mode Fibre Using Direct Detection", International OFDM Workshop 2008

[43] W.R. Peng, X. Wu, V.R. Arbab, B. Shamee, J.Y. Yang, L.C. Christen, K.M. Feng, A.E. Willner, and S. Chi, "Experimental demonstration of 340 km SSMF transmission using a virtual single sideband OFDM signal that employs carrier suppressed and iterative detection techniques," in Proc. OFC 2008, paper OMU1

[44] Z. Zan, M. Premaratne, and A.J. Lowery, "Laser RIN and linewidth requirements for direct detection optical OFDM," in Proc. OFC 2008, paper CWN2

[45] W. Shieh, X. Yi, and Y. Tang, "Transmission experiment of multi-gigabit coherent optical OFDM systems over 1000 km SSMF fibre," Electron. Lett., vol. 43, no. 3, pp. 183-184, 2007

[46] W. Shieh, C. Athaudage, "Coherent optical orthogonal frequency division multiplexing," Electronics Letters, 2006

[47] S.L. Jansen, "16x52.5-Gb/s, "50-GHz spaced, POLMUX-CO-OFDM transmission over 4,160 km of SSMF enabled by MIMO processing", in Proc. ECOC 2007

[48] W. Shieh, I. Djordjevic, "OFDM for Optical Communications", Elsevier Inc., 2010

[49] L. A. Buckman, B. E. Lemoff, A. J. Schmit, R. P. Tella, and W. Gong, "Demonstration of a small-form-factor WWDM transceiver module for 10-Gb/s local area networks," IEEE Photon. Technol. Lett., vol. 14, no. 5, pp. 702-704, 2002

[50] F. Buchali et al., "Optical OFDM: A promising high-speed optical transport technology," Bell Labs Technical Journal archive, vol. 14, iss. 1, 2009

[51] A.J. Lowery, "Improving sensitivity and spectral efficiency in direct-detection optical OFDM systems," in Proc. OFC 2008, paper OMM4

[52] D. Qian, N. Cvijetic, J. Hu, T. Wang, "Optical OFDM transmission in metro/access networks," in Proc. OFC 2009, paper OMV1

[53] M. Ruffini, D. Mehta, B. O'Sullivan, L. Quesada, L. Doyle, "Deployment Strategies for Protected Long-Reach PON," J. Opt. Commun. Netw., vol. 4, pp. 118-129, 2012.

[54] D. B. Payne and R. P. Davey, "The future of fibre access systems?," BT Technol. J., vol. 20, pp. 104-114, 2002.

[55] K. Kanonakis, I. Tomkos, H. G. Krimmel, F. Schaich, C. Lange, E. Weis, J. Leuthold, M. Winter, S. Romero, P. Kourtessis, M. Milosavljevic, I. Cano and J. Prat, "An OFDMA-Based Optical Access Network Architecture Exhibiting Ultra-High Capacity and Wireline-Wireless Convergence," IEEE Communications Magazine, vol. 50, no. 8, pp. 71-78, 2012

[56] D.-Z. Hsu, C.-C. Wei, H.-Y. Chen, W.-Y. Li, J. Chen, "Long-reach OFDM PON," OptoeElectronics and Communications Conference (OECC), pp. 34 - 36, 2011

[57] L. Xiang, S. Chandrasekhar, B. Zhu, P. J. Winzer, and D. W. Peckham, "7×224-Gb/s WDM Transmission of Reduced-Guard-Interval CO-OFDM with 16-QAM Subcarrier Modulation on a 50-GHz Grid over 2000 km of ULAF and Five ROADM Passes," in Proc. European Conference on Optical Communication (ECOC), 2010, paper Tu.3.C.2

[58] D. Qian, M.-F. Huang, E. Ip, Y.-K. Huang, Y, Shao, J. Hu, and T. Wang, "High Capacity/Spectral Efficiency 101.7-Tb/s WDM Transmission Using PDM-128QAM-OFDM Over 165-km SSMF Within C- and L-Bands," IEEE J. Lightwave Technol., vol. 30, pp. 1540-1548, 2012

[59] L. Stampoulidis, M. F. O'Keefe, E. Giacoumidis, et al., "Fabrication of the first high-speed GaAs IQ electro-optic modulator arrays and applicability study for low-cost Tb/s direct-detection optical OFDM networks", OFC/NFOEC, 2013, paper OW1G.4

[60] D. P. Shea and J. E. Mitchell, "10-Gb/s 1024-Way-Split 100-km Long-Reach Optical-Access Network," IEEE J. Lightwave Technol., vol. 25, no. 3, pp. 685-693, 2007.

[61] Analysys Mason, final report for the broadband stakeholder group, “The cost of deploying fibre-based next-generation broadband infrastructure,” report commissioned by the Broadband Stakeholder Group with support from the Department for Business Enterprise & regulatory reform (2008).

6 Abbreviations

ALUD	Alcatel-Lucent Deutschland AG
APD	Avalanche Photo Diode
ASE	Amplified Spontaneous Emissions
ASTON	Aston University
ATESIO	Atesio GMBH
AWG	Arrayed Waveguide Grating
BER	Bit Error Rate
BiPON	Bit-Interleaving Multiplexing PON
BMRx	Burst-Mode Receiver
BW	Bandwidth
CAPEX	Capital Expenditure
C-band	Band in the wavelength range 1530–1565 nm
CD	Chromatic Dispersion
CO	Central Office
CO-OFDM	Coherent OFDM
COR	Coriant GmbH
CPE	Customer Premises Equipment
CTLE	Continuous Time Linear Equalizer
D/S	Downstream
DACs/ADCs	Digital-to-Analogue/Analogue-to-Digital Converters
DBA	Dynamic Bandwidth Assignment
DBR	Distributed Bragg Reflector
DCF	Dispersion Compensating Fibre
DD-OOFDM	Direct-Detection Optical OFDM
DFB	Distributed Feedback
DFE	Decision Feedback Equalizer
DISCUS	The DIStributed Core for unlimited bandwidth supply for all Users and Services
DP	Distribution Point
D-side	Distribution side
DSP	Digital Signal Processer
DUT	Device Under Test

DWDM	Dense Wavelength Division multiplexer
ECL	External Cavity Laser
EDC	Electronic Dispersion Compensation
EDFA	Erbium Doped Fibre Amplifier
EPON	Ethernet Passive Optical Network
E-side	The access network from the local Exchange sidesite to the cabinet location
FEC	Forward Error Correcting
FFE	Feedforward Equalizer
FFT	Fast Fourier Transform
FSR	Free Spectral Range
GPON	Gigabit Passive Optical Network
IFFT	Inverse Fast Fourier Transform
III-V	III V Lab GIE
IL	Insertion Loss
IM/DD	Intensity Modulation/Direct Detection
IMEC	Interuniversitair Micro-Electronica Centrum VZW
IQ	In-phase Quadrature-phase
ISI	Inter-symbol Interference
ITU	International Telecommunications Union
ITU-T	ITU's Telecommunication Standardization Sector
KTH	Kungliga Tekniska Hoegskolan
L-band	Band in the wavelength range 1565–1625 nm
LBMRx	Linear Burst-Mode Receiver
LDPC	Low-Density Parity-Check
LE	Local Exchange
LMS	Least Mean Square
LO	Local Oscillator
LPF	Low-Pass Filters
LR-PON	Long Reach Passive Optical Network
MAC	Media Access Control
MC	Metro-core
MGY	Modulated Grating Y-branch
MIMO	Multiple-input Multiple-output

MLSE	Maximum Likelihood Sequence Estimation
MZM	Mach-Zehnder modulator
NG-PON2	Next Generation PON Stage 2
NRZ	Non Return to Zero
ODN	Optical Distribution Network
OEO	Optical-Electronic-Optical (conversion)
OFDM	Orthogonal Frequency Division Multiplexing
OLT	Optical Line Termination
OMCI	ONT Management and Control Interface
ONU	Optical Network Unit
OOFDM	Optical OFDM
OOK	On-off keying
OPP	Optical Path Penalty
OSNR	Optical signal to Noise Ratio
OTG	Optical Transceiver Group
OTR	optical-to-RF
p2p	Point-to-Point
PAPR	Peak-to-Average Power Ratio
PCT	Paired Channel Technology
PIN-Rx	Positive Intrinsic Negative Receiver (Receiver with PIN photodiode)
PLOAM	Physical Layer Operations, Administration and Maintenance
PMD	Polarization Mode Dispersion
POLATIS	Polatis Ltd
PON	Passive Optical Network
PP	Restricted to other programme partners (including Commission Services)
PtP	Point-to-Point
PU	Public
QAM	Quadrature Amplitude Modulation
RB	Rayleigh backscattering
RE	Restricted to a group specified by the consortium (including Commission Services)
RF	Radio Frequency

RLS	Recursive Least Squares
ROADM	Re-configurable Optical Add Drop Multiplexer
RTO	RF-to-optical
SE	Spectral Efficiency
SFP	Slotted Fabry-Perot
SNR	Signal to Noise Ratio
SOA	Semiconductor Optical Amplifiers
SSB	Single Sideband
SSMF	Standard Single Mode Fiber
STM	Synchronous Transport Module
TCD	Trinity College Dublin
TDMA	Time Division Multiple Access
TDM-PON	Time division Multiplexed Passive Optical Network
TI	Telecom Italia S.p.A
TID	Telefonica Investigacion Y Desarrollo SA
U/S	Upstream
UCC	University College Cork
UDWDM	Ultra Dense WDM
VOA	Variable Optical Attenuator
WDM	Wavelength Division Multiplexing
WDM-PON	Wavelength Division Multiplexed Passive Optical Network
WOLA	Weighted OverLay and Add
WSS	Wavelength Selective Switch